Available online at www.sciencedirect.com
SCIENCE DIRECT®
Precambrian Research 147 (2006) 193–222
Precambrian Research
www.elsevier.com/locate/precamres

# Paleomagnetic record of Africa and South America for the 1200–500 Ma interval, and evaluation of Rodinia and Gondwana assemblies

Eric Tohver[a,b,*], Manoel S. D'Agrella-Filho[b], Ricardo I.F. Trindade[b]

[a] Centro de Pesquisas Geocronológicas, Instituto de Geociências, Universidade de São Paulo, Rua do Lago 562, 05508-080 São Paulo, Brazil
[b] Departamento de Geofísica, Instituto de Astronomia, Geofísica e Ciências Atmosféricas, Universidade de São Paulo, Rua do Matão 1226, 05508-090 São Paulo, Brazil

Received 16 March 2005; received in revised form 20 October 2005; accepted 6 January 2006

**Abstract**

At least two supercontinents – Rodinia and Gondwana – have been proposed for the 1200–500 Ma time interval on the basis of stratigraphic, geochronological and paleomagnetic grounds. Although the exact configuration of Rodinia is still a matter of debate, both supercontinents are linked insofar as the demise of the older Rodinia begat the younger Gondwana. In order to constrain the paleogeographic transition between these two supercontinents, we evaluate an updated paleomagnetic database (148 poles) for Africa together with unpublished data from South America, using the *Q*-factor criteria of Van der Voo [Van der Voo, R., 1990. The reliability of paleomagnetic data. Tectonophysics 184, 1–9]. A postulated Grenvillian suture between Laurentia and the united Amazonia–West Africa craton is supported by comparing the Meso-Neoproterozoic drift history of these two cratons. Comparing this drift history with that of the remaining West Gondwanan cratonic elements: São Francisco–Congo, Kalahari, Rio de Plata, and Arabian–Nubian shield, reveals that these cratons were not part of Rodinia. The contrasting drift history of Laurentia cum Amazonia–West Africa with "central" West Gondwanan cratons São Francisco–Congo, Kalahari suggests the continued existence of at least two separate tectonic plates separated by an ocean basin. The assembly of central Gondwana, i.e. Kalahari, São Francisco–Congo, and the Arabia–Nubian shield was completed during latest Neoproterozoic times, as indicated by the approximation of ca. 550 Ma paleomagnetic poles. The collision of these central Gondwanan blocks with the Amazonia–West Africa craton appears to have occurred by mid-Cambrian times, after the opening of the Iapetus ocean basin between Laurentia and Amazonia–West Africa. We propose a scenario in which West Gondwana was formed through at least two distinct orogenic episodes: terranes and cratons accreting to the São Francisco–Congo craton in a series of collisions from 940 to 550 Ma, followed by the collision with Amazonia–West Africa and minor contiguous blocks (Rio Apa and Pampia) at ca. 520 Ma. West Gondwana was not a coherent tectonic unit before the end of Precambrian times, with a major mobile belt separating at least two separate continental masses.


*Keywords:* Proterozoic; Paleomagnetism; Rodinia; West Gondwana; Amazon; West Africa; Kalahari; São Francisco; Congo; Arabia–Nubia

## 1. Introduction

Paleomagnetic investigations of the Precambrian era have been at the heart of many long-standing arguments regarding how much of early Earth history can be reliably described by uniformitarian principles. Inferences about deep Earth processes during the Precambrian

* Corresponding author.
*E-mail address:* etohver@usp.br (E. Tohver).

0301-9268/$ – see front matter © 2006 Published by Elsevier B.V.
doi:10.1016/j.precamres.2006.01.015

are drawn from paleomagnetic data; examples include absolute time constraints on the initiation of the geodynamo (Layer et al., 1996) and the long term geometric attributes of the terrestrial field (Kent and Smethurst, 1998) imparted by a differentiated core with stable convection patterns established in the outer core (Merrill and McFadden, 1995). The absolute, global reference frame implicit to paleomagnetic data is ideal for documenting the history and dynamics of the plate tectonic regime (Van der Voo and Meert, 1991; Meert et al., 1993). Non-uniformitarian alternatives to the plate tectonic regime, such as the subduction-free, ensialic orogeny (Piper, 1976, 1983; Kröner, 1977), or the possibility of pan-lithospheric drift (i.e. true polar wander) occurring outside of a plate tectonic framework (Goldreich and Toomre, 1969), commonly rely on paleomagnetic data for support (Kirschvink et al., 1997; Evans, 1998) or repudiation (Meert, 1999; Torsvik et al., 2001). The more conventional debate over paleogeography for the Proterozoic relies heavily on the paleomagnetic record, especially given the breakdown in the traditional link between paleoclimatic indicators and paleolatitude engendered by the Snowball Earth hypothesis (Hoffman et al., 1998; Williams and Schmidt, 2000).

The review of paleomagnetic data for West Gondwana presented here is part of an ongoing reassessment of Proterozoic paleogeography being undertaken by many workers (e.g. Weil et al., 1998; D'Agrella-Filho et al., 1998; Pesonen et al., 2003; Meert, 2003; Meert and Torsvik, 2003; Pisarevsky et al., 2003). The renewal of interest in the paleomagnetic record from the Precambrian focuses chiefly on two controversial hypotheses that have come to dominate discussion of the late Mesoproterozoic to Cambrian interval of Earth history: the Rodinia supercontinent (cf. Paleopangea of Piper, 1980, 2000) and the snowball Earth hypothesis invoked to explain Neoproterozoic glacial deposits at low latitudes (Kirchvink, 1992; Meert and Van der Voo, 1994), as reviewed recently by Evans (2000) and Meert and Torsvik (2004). On the paleographic front, a recent review of the geochronological and paleomagnetic data from India, Australia, Antarctica, and eastern Africa challenges the classical view of a long-standing, united East Gondwana (Meert, 2003). In contrast, the tectonic models for West Gondwana, especially the South American units – Amazon, Rio de la Plata, Luis Alves, and São Francisco cratons and their intervening mobile belts – have not benefited from uniform scrutiny of the paleomagnetic database. In this contribution, we present new, previously unpublished data from South America, as well as a comprehensive review of the existing South American and African databases. In the time elapsed since the last review of the African database (Van der Voo and Meert, 1991), new paleomagnetic and geochronological data have been reported, allowing for an updated reassessment of the paleogeography of the constituents of West Gondwana (Fig. 1). We have chosen the time interval 1200–500 Ma as appropriate for our review, as this interval covers the proposed assembly and break-up of the Rodinia supercontinent, as well as the subsequent assembly of Gondwana, thus providing the reference frame of a unifying paleogeographic model.

## 2. Paleomagnetic database and selection criteria

In conducting this review, we have gathered together data from articles published in standard journals with an international audience, in addition to "grey" literature sources such as regional journals, PhD theses, and meeting abstracts. Some of the data assembled from this process were deemed fit for inclusion in the subsequent discussion of paleogeography, while others have been excluded from construction of the individual apparent polar wander paths (APWP) for each craton. The philosophy underlying our selection process and the (admittedly) skeletal APWPs that emerge differs from other recent reviews of the Precambrian database (e.g. Buchan et al., 1994, 2001), where more stringent criteria are used to exclude all but a few paleomagnetic "key poles." The "key pole" approach emphasizes the reliability of those paleopoles that are privileged by more precise geochronological data and/or field tests suggestive of a primary remanence. One would expect that paleogeographic reconstructions based exclusively on "key poles" would be somehow more reliable. Alas, a consequence of the more conservative approach to paleomagnetic data is that paleogeographic reconstructions themselves are much more loosely constrained. A number of factors contribute: the lack of "reliable" data and the consequently long and frequent hiatuses in the drift record, the uncertain polarity of pre-Jurassic paleomagnetic data, and the mismatch in ages in comparing acceptable paleopoles from different cratons. It is our contention that paleogeographic reconstructions based on the APWP approach present a more realistic approximation of a continuous geological drift history, even where certain portions of the path are based on individual poles that cannot be verified by field tests or precise geochronology. In short, data that are not demonstrably good are not necessarily bad data. Excluding such data a priori runs the risk of eliminating accurate recorders of the geomagnetic field and, incidentally, discourages present and future workers from further refining or revisiting these results.

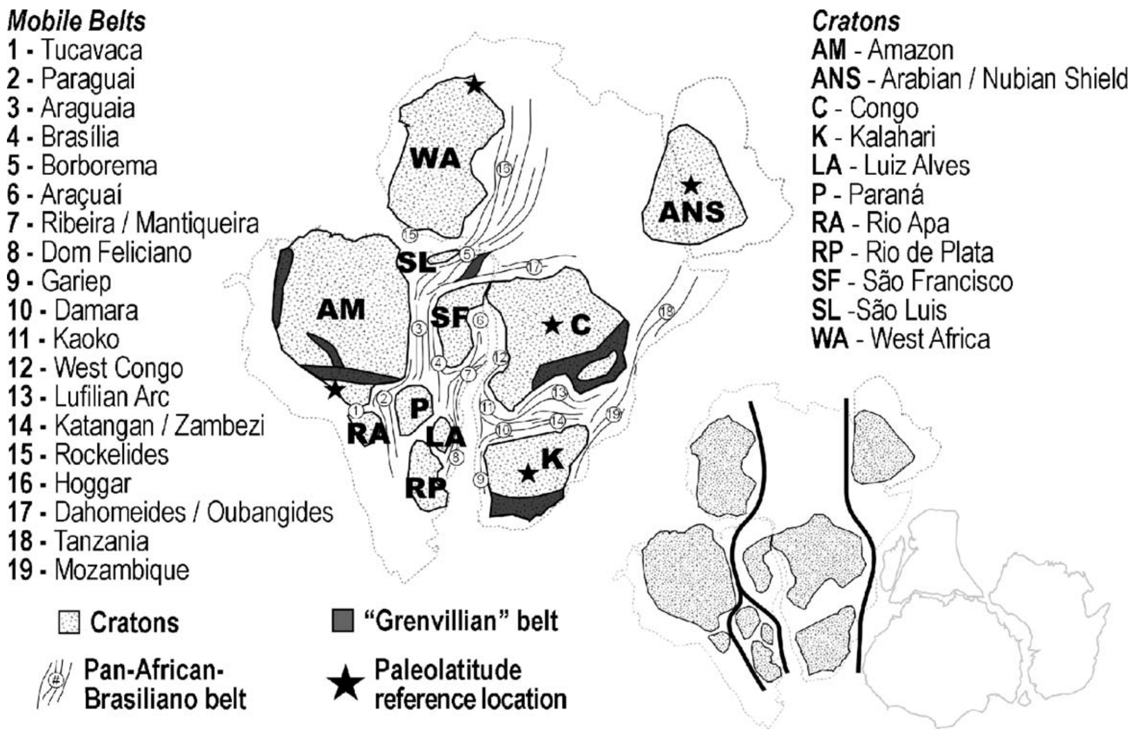


Fig. 1. *Main*: Map of the restored geometry of the western Gondwana cratonic blocks and intervening Pan-African/Brasiliano mobile belts, following the reconstruction parameters of Lawver and Scotese (1987). Note that alternative fits for West Africa and Amazonia proposed on the basis of Paleoproterozoic paleomagnetic data (Onstott and Hargraves, 1981; Nomade et al., 2003) and that Phanerozoic deformation internal to Africa (Fairhead, 1988) would result in relatively minor shifts in relative paleogeographic position and paleomagnetic pole positions for the Precambrian. The locations of "Grenvillian" belts are depicted with grey shading: NW Amazon craton, Columbia (Restrepo-Pace et al., 1997); Ji-Parana shear zone network and Nova Brasilândia metasedimentary belt, SW Amazon craton, Brazil (Tohver et al., 2004a, 2005a,b); Carirís Velhos belt, NE São Francisco craton, Brazil (Neves, 2003); SE Congo craton, Mozambique belt (Hanson, 2003); S Kalahari craton, Namaqua-Natal belt (Hanson, 2003). Inset: Simplified map of all of Gondwana, showing the location of prominent suture zones that mark the welding together of far-flung cratonic blocks of East Gondwana, the central "spine" of the São Francisco–Congo and Kalahari cratons, and the westernmost blocks, dominantly the conjoined West Africa-Amazon craton.

In compiling the database for the West Gondwana tectonic elements, we have grouped poles by cratonic units (Fig. 1), comprising the Kalahari (K), Congo (C), São Francisco (SF), West Africa (W), Amazon (A), Rio de la Plata (RP), and Luis Alves (LA). For poles obtained from the surrounding mobile belts, we have incorporated the data into the craton database when structural continuity with the relevant craton could be established. Otherwise, poles have entered the Panafrican/Brasiliano Belts list (B), together with poles obtained on terranes that constitute the Arabian–Nubian shield (N), in consideration of its accretionary, non-cratonic history (Stern, 1994; Windley et al., 1996).

Table 1 lists poles for all of the West Gondwana cratonic blocks rotated to Africa coordinates using the Euler pole rotation parameters of Lawver and Scotese (1987). An alternative fit between West Africa and Amazon proposed by Onstott and Hargraves (1981) differs slightly in the relative position of these two cratons in their pre-Gondwanan position, but is still in keeping with our general conclusions. The South American portion of the database includes many results from regional journals, doctoral theses, and assorted abstracts that were previously unavailable to a wide readership. Old paleomagnetic results have been updated with new geochronological results, where available, in order to better constrain the age of paleomagnetic poles. Results that have been superseded by later studies have been noted as such. Each entry in the compilation has been assessed using $Q$-factor criteria outlined by Van der Voo (1990). Briefly stated, the $Q$-factor is a numerical index to the reliability of paleomagnetic data based on whether or not the reported data for that unit includes the following tests: (1) the presence of good age constraints for the rock unit and the presumption that this approximates the age of the magnetization, (2) a statistically precise magnetic direction obtained through analysis of an adequate number of samples over a significant geographic area, (3) detailed demagneti-

Table 1

| | Craton/belt | Age | | Direction | | Paleomagnetic pole | | | | Precision | | | | Quality index | | | | | | | Q | Reference |
|---|---|---|---|---|---|---|---|---|---|---|---|---|---|---|---|---|---|---|---|---|---|---|
| | | Minimum | Maximum | Declination | Inclination | Plat | Plon | N | n | dp | dm | K | A95 | 1 | 2 | 3 | 4 | 5 | 6 | 7 | | |
| Kalahari | | | | | | | | | | | | | | | | | | | | | | |
| K1 | Ezelsfontein formation | 1178 | 1300 | 29 | −11 | **54** | **77** | 1 | *3* | 9 | 17 | 54 | 17 | 0 | 0 | 0 | 0 | 1 | 0 | 0 | **1** | 1, 2[a] |
| **K2** | **Premier Mine kimberlite** | 1170 | 1220 | 186 | −25 | **51** | **38** | 2 | *16* | 4 | 8 | 26 | 7 | 1 | 0 | 0 | 1 | 1 | 0 | 0 | **3** | 3, 4[a] |
| K3 | Premier Kimberlite | 1155 | 1175 | 165 | −3 | **59** | **358** | 1 | *2* | 1 | 3 | 453 | 3 | 0 | 0 | 0 | 0 | 0 | 0 | 1 | **1** | 4, 5[a] |
| **K4** | **Franspoort Kimberlite** | 1150 | 1223 | 193 | −24 | **49** | **49** | 1 | *5* | 8 | 8 | 54 | 11 | 1 | 1 | 0 | 0 | 0 | 0 | 1 | **3** | 5 |
| **K5** | **Schuller Kimberlite** | 1150 | 1223 | 203 | −44 | **33** | **54** | 1 | *8* | 6 | 6 | 101 | 6 | 1 | 1 | 0 | 0 | 0 | 0 | 1 | **3** | 5 |
| **K6** | **National Kimberlite** | 1124 | 1156 | 221 | −51 | **−21** | **245** | 1 | *11* | 7 | 10 | 41 | 7 | 1 | 0 | 0 | 0 | 1 | 0 | 1 | **3** | 6 |
| **K7** | **Premier Combined** | 1155 | 1175 | – | – | **41** | **55** | 4 | *29* | 16 | 16 | – | 16 | 1 | 1 | 1 | 0 | 1 | ? | 1 | **5** | 7 |
| K8 | Montrose Kimberlite | 1000 | 1300 | 193 | 11 | **66** | **62** | 1 | *1* | – | – | 373 | 3 | 0 | 0 | 0 | 0 | 0 | 0 | 1 | **1** | 4, 5[a] |
| K9 | Barby Lavas, Sinclair Gp. | 1098 | 1217 | 4 | −7 | **68** | **28** | 19 | *98* | – | – | 5 | 17 | 1 | 0 | 0 | 1 | 0 | 1 | 0 | **3** | 8, 9[a], 15[a] |
| K10 | Guperas Fm, Sinclair Gp. | 1000 | 1150 | 336 | −20 | **63** | **317** | 4 | *16* | 2 | 3 | 87 | 3 | 0 | 0 | 0 | 0 | 1 | 0 | 0 | **1** | 8 |
| K11 | Mashonaland Dolerites | 1103 | 1107 | 183 | −10 | **65** | **43** | 10 | *79* | 4 | 7 | 50 | 6 | 0 | 0 | 0 | 0 | 0 | 0 | 0 | **0** | 11, 15[a] |
| **K12** | **Post−Waterberg diabases** | 1103 | 1107 | 190 | 2 | **65** | **51** | 13 | *90* | 5 | 5 | 31 | 8 | 1 | 1 | 0 | 1 | 1 | 1 | 0 | **5** | 12, 13[a], 15[a] |
| **K13** | **Timbavati Gabbros** | 1112 | | 187 | −5 | **63** | **47** | 7 | *27* | 3 | 3 | 209 | 5 | 1 | 1 | 1 | 0 | 1 | 0 | 0 | **4** | 14, 15[a] |
| **K14** | **Umkondo Dolerite/Gabbro** | 1103 | 1107 | 178 | −12 | **64** | **28** | 9 | *98* | 4 | 8 | 20 | 8 | 0 | 1 | 1 | 0 | 1 | 0 | 0 | **3** | 15[a], 16 |
| **K15** | **Umkondo combined**[b] | 1103 | 1107 | – | – | **64** | **36** | 67 | *315* | – | – | – | 4 | 1 | 1 | 1 | 1[b] | 1 | 1 | 1 | **7** | 15 |
| K16 | Auborus Fm. | 800 | 1000 | 163 | −33 | **43** | **354** | 8 | *37* | 7 | 13 | 24 | 12 | 0 | 0 | 0 | 0 | 1 | 0 | 0 | **1** | 8 |
| **K17** | **Kalkpunt Fm. (Koras Gp.)** | 800 | 1050 | 170 | −7 | **57** | **3** | 9 | *25* | 4 | 7 | 67 | 7 | 0 | 1 | 1 | ? | 1 | 1 | 0 | **4** | 1 |
| K18 | Ntimbankulu Pluton | 1030 | 1060 | 306 | 13 | **27** | **327** | 6 | *32* | 9 | 18 | 14 | 18 | 1 | 0 | 0 | 0 | 1 | 0 | 0 | **2** | 17, 18[a] |
| K19 | Port Edward Charnockite | 999 | 1009 | – | – | **−7** | **328** | 4 | *37* | – | – | 356 | 4 | 1 | 1 | 1 | 0 | 0 | 0 | 0 | **3** | 19 |
| K20 | O'Okiep basic intrusions | 990 | 1050 | 132 | −48 | **15** | **335** | 5 | *22* | 13 | 19 | 28 | 15 | 1 | 0 | 1 | 0 | 0 | 0 | 0 | **2** | 2[a], 8 |
| **K21** | **Namaqua metamorphics** | 980 | 1020 | – | – | **8** | **330** | 9 | *44* | – | – | – | 11 | 1 | 1 | 1 | 0 | 0 | 1 | 0 | **4** | 2, 20 |
| K22 | Klein Karas Dikes | 846 | 928 | 290 | −7 | **20** | **294** | 4 | *12* | 18 | 35 | 5 | 35 | 0 | 0 | 1 | 0 | 0 | 0 | 1 | **2** | 2[a], 8 |
| K23 | Florida + Kalkpunt Fm. | 750 | 850 | 93 | −8 | **1** | **297** | 4 | *11* | 7 | 14 | 84 | 14 | 0 | 0 | 0 | 0 | 0 | 1 | 1 | **2** | 1, 13[a], 21[a] |
| K24 | L. Nama Gp. n1 | 600 | 700 | 20 | −11 | **61** | **63** | 20 | 75 | 7 | 13 | 8 | 13 | 0 | 0 | 1 | 0 | 1 | 1 | 0 | **3** | 22, 27[c], 23[a], 24 |
| K25 | Pre-Nama Dikes[d] | 583 | 723 | 357 | −53 | **85** | **228** | | *28* | 21 | 30 | 13 | 22 | 0 | 0 | 0 | 0 | 0 | 0 | 0 | **0** | 8, 25[a] |
| K26 | Gannakouriep Dikes | 706 | 728 | 93 | 64 | **−22** | **67** | 2 | *13* | | – | – | – | 1 | 0 | 1 | 0 | 0 | 0 | 0 | **2** | 25[a], 26 |
| K27 | Upper Nama Gp. n2 | 550 | 600 | 87 | 31 | **5** | **271** | 4 | *15* | 9 | 17 | 41 | 15 | 0 | 0 | 1 | 0 | 1 | 1 | 1 | **4** | 22, 27[c], 23[a], 24 |
| K28 | Gannakouriep remag. | 538 | 546 | 339 | 36 | **37** | **353** | 2 | *6* | 5 | 9 | 72 | 8 | 1 | 0 | 1 | 0 | 0 | 0 | 1 | **3** | 25[a], 26 |
| K29 | Fish River (recalculated) | 530 | 600 | – | – | **−5** | **323** | 5 | *26* | – | – | – | – | 0 | 0 | 0 | 0 | 1 | 0 | 1 | **2** | 9, 27[c] |
| **K30** | **Equeefa Dikes/Mzumbe gneiss** | 530 | | – | – | **25** | **17** | 8 | *98* | – | – | – | 11 | 1 | 1 | 1 | 0 | 1 | 0 | 0 | **4** | 19 |
| K31 | Doornpoort Fm. | 500 | 550 | 229 | −43 | **22** | **65** | 6 | *28* | 7 | 11 | 58 | 9 | 0 | 1 | 0 | −1 | 0 | 0 | 1 | **1** | 8 |
| K32 | Sijarira Group | 488 | 600 | 291 | 67 | **2** | **352** | 5 | *40* | 26 | 30 | 9 | 19 | 0 | 0 | 0 | 1 | 1 | 0 | 1 | **3** | 28 |
| K33 | Lower Nama Group n3 | 450 | 550 | 122 | −67 | **−4** | **344** | 6 | *22* | 19 | 23 | 25 | 14 | 0 | 0 | 0 | 0 | 0 | 0 | 0 | **0** | 22, 27[c], 23[a], 24 |
| K34 | Nama Group n1 | 450 | 550 | 7 | −22 | **−73** | **228** | 6 | *25* | 16 | 16 | 15 | 18 | 0 | 1 | 0 | 0 | 0 | ? | 0 | **1** | 27 |
| K35 | Nama Group n2 | 450 | 550 | 265 | −25 | **−1** | **271** | 8 | *51* | 19 | 19 | 7 | 24 | 0 | 1 | 0 | 0 | 0 | ? | 0 | **1** | 27 |
| K36 | Nama Group n3 | 450 | 550 | 356 | 52 | **30** | **14** | 4 | *25* | 25 | 25 | 24 | 19 | 0 | 1 | 0 | 0 | 0 | ? | 0 | **1** | 27 |
| K37 | Nama Group n4 | 450 | 550 | 330 | 2 | **50** | **327** | 6 | *30* | 16 | 16 | 15 | 18 | 0 | 1 | 0 | 0 | 0 | ? | 0 | **1** | 27 |
| **K38** | **Nama Group n5 composite** | 450 | 550 | – | – | **−17** | **318** | 11 | *42* | – | – | – | 10 | 0 | 1 | 1 | 0 | 1 | 0 | 0 | **3** | 27 |
| K39 | Nama Group n5 (untilted) | 450 | 550 | 69 | −42 | **−28** | **303** | 5 | *20* | 13 | 13 | 30 | 14 | 0 | 0 | 0 | ? | 0 | ? | 0 | **0** | 27 |
| K40 | Blaubeker Fm. | 445 | 497 | 344 | 23 | **51** | **353** | 3 | *11* | 11 | 20 | 45 | 19 | 0 | 0 | 0 | 0 | 0 | 0 | 0 | **0** | 22, 27[c], 23[a], 24 |

| | | | | | | | | | | | | | | | | | | | | | | |
|---|---|---|---|---|---|---|---|---|---|---|---|---|---|---|---|---|---|---|---|---|---|---|
| Conho | | | | | | | | | | | | | | | | | | | | | | |
| C1 | Kisii Lavas[e] | 2529 | 2533 | – | – | **6** | **348** | | | – | – | 24 | 11 | 0 | 1 | 0 | 0 | 1 | 0 | 0 | **2** | 29, 30[a] |
| C2 | Bukoban Sandstone[e] | >1282 | | 132 | −19 | **40** | **317** | | *1* | 12 | 11 | 21 | 20 | 0 | 0 | 0 | 0 | 1 | 0 | 1 | **2** | 31, 32[a] |
| C3 | Cunene Anorthosite[e] | 1366 | 1374 | – | – | **3** | **75** | 16 | *77* | – | – | – | – | 0 | 0 | 0 | 0 | 0 | 1 | 1 | **2** | 33, 34[a] |
| **C4** | **Post-Kibaran intrusives** | 1212 | 1248 | 108 | 16 | **17** | **293** | 11 | *49* | – | – | 7 | 7 | 1 | 1 | 1 | 0 | 1 | 0 | 0 | **4** | 35 |
| C5 | Gabon Dikes | 963 | 1010 | 262 | −49 | **−8** | **252** | 4 | *13* | 33 | 33 | 13 | 27 | 0 | 0 | 1 | 0 | 0 | 1 | 1 | **3** | 36 |
| C6 | Nyabikere Massif | 920 | 980 | 46 | −29 | **−43** | **317** | 1 | *4* | 9 | 15 | 25 | 14 | 1 | 0 | 1 | 0 | 0 | 0 | 0 | **2** | 35 |
| C7 | Abercorn Sandstone | 900 | 1200 | 319 | −14 | **49** | **300** | 1 | *5* | 8 | 16 | 26 | 15 | 0 | 0 | 0 | 0 | 1 | 0 | 1 | **2** | 33 |
| C8 | Kigonero Flags | 900 | 1200 | 281 | −47 | **−12** | **93** | 4 | *20* | 22 | 35 | 13 | 27 | 0 | 0 | 0 | 0 | 1 | 0 | 1 | **2** | 31, 32[a] |
| C9 | Malagarasi Sandstone | 900 | 1200 | 263 | −16 | **7** | **112** | 1 | *12* | 13 | 26 | 5 | 26 | 0 | 0 | 0 | 0 | 1 | 0 | 1 | **2** | 33 |
| C10 | Mbala Dolerites | 900 | 1000 | 84 | 40 | **2** | **98** | 2 | *16* | 13 | 22 | 19 | 18 | 0 | 0 | 0 | 0 | 1 | 0 | 1 | **2** | 33 |
| C11 | Ikorongo Group | 850 | 1000 | 132 | 53 | **−35** | **84** | 6 | *31* | 19 | 27 | 13 | 19 | 0 | 0 | 0 | 0 | 1 | 0 | 1 | **2** | 33 |
| **C12** | **Gagwe/Kabuye Lavas** | 788 | 835 | 241 | −39 | **25** | **93** | 12 | *80* | 7 | 12 | 18 | 10 | 0 | 1 | 1 | 0 | 1 | 0 | 1 | **4** | 32[a], 37 |
| **C13** | **Gagwe Lavas** | 788 | 835 | 239 | −25 | **29** | **103** | 28 | *153* | 7 | 14 | 5 | 13 | 0 | 1 | 0 | 0 | 1 | 0 | 1 | **3** | 31, 32[a] |
| **C14** | **Bukoban Intrusives** | 750 | 850 | 77 | 32 | **11** | **101** | 16 | *76* | 12 | 22 | 5 | 19 | 1 | 0 | 0 | 0 | 1 | 1 | 1 | **4** | 33 |
| C15 | Mbozi Mafic Complex | 713 | 773 | 10 | 11 | **72** | **68** | 7 | *19* | 9 | 19 | 19 | 18 | 1 | 0 | 0 | 0 | 0 | 1 | 0 | **2** | 33 |
| **C16** | **Mbozi Mafic Complex HT** | 713 | 773 | 320 | 16 | **46** | **325** | 10 | *64* | 5 | 9 | 32 | 9 | 0 | 1 | 1 | 0 | 1 | 1 | 1 | **5** | 32[a], 37 |
| **C17** | **Nosib Group nq1 HT** | 742 | 746 | 312 | 40 | **28** | **323** | 6 | *25* | 11 | 18 | 21 | 15 | 0 | 1 | 1 | ? | 1 | 0 | 1 | **4** | 38, 39, 40[a], 41 |
| C18 | Chela Gp. Volcaniclastics | 742 | 746 | 311 | 49 | **23** | **329** | 4 | *21* | 37 | 37 | 15 | 34 | 0 | 0 | 1 | 0 | 1 | 0 | 0 | **2** | 39, 40 and 41[a] |
| C19 | Plateau Series | 700 | 1000 | 159 | −72 | **22** | **19** | 2 | *15* | 61 | 70 | 4 | 40 | 0 | 0 | 0 | 0 | 0 | 0 | 0 | **0** | 33 |
| C20 | Lower Buanji Series[d] | 700 | 1000 | 358 | −20 | **87** | **263** | 6 | *25* | 5 | 9 | 60 | 9 | 0 | 1 | 0 | 0 | 1 | 0 | −1 | **1** | 33 |
| C21 | Lower Plateau Series | 700 | 1000 | 13 | −41 | **71** | **173** | | *31* | 12 | 19 | 19 | 15 | 0 | 1 | 0 | 0 | 1 | 0 | 0 | **2** | 33 |
| C22 | Mpulungu Plateau Series | 700 | 1000 | 85 | −69 | **10** | **172** | 2 | *8* | 14 | 16 | 70 | 10 | 0 | 0 | 0 | 0 | 1 | 0 | 0 | **1** | 33 |
| C23 | Upper Plateau Series | 700 | 1000 | 177 | −37 | **60** | **25** | 3 | *13* | 9 | 15 | 90 | 13 | 0 | 0 | 0 | 0 | 1 | 1 | 0 | **2** | 33 |
| C24 | Nosib Group nq2 IT | 660 | 744 | 12 | 36 | **51** | **33** | 7 | *28* | 8 | 14 | 26 | 12 | 0 | 1 | 1 | ? | 1 | 1 | 0 | **4** | 38, 40[a], 41 |
| C25 | Manyovu Redbeds | 650 | 795 | 246 | −2 | **22** | **117** | 5 | *44* | 20 | 40 | 5 | 40 | 0 | 0 | 0 | 0 | 1 | 1 | 1 | **3** | 32[a], 33 |
| C26 | Chuos Fm, Otavi Gp. dc1 | 635 | 746 | 354 | 34 | **52** | **6** | 4 | *15* | 23 | 40 | 8 | 35 | 0 | 0 | 1 | ? | 0 | 1 | 0 | **2** | 38, 40[a], 41 |
| C27 | Chuos Fm, Otavi Gp. dc2 | 635 | 746 | 336 | −65 | **55** | **224** | 10 | *26* | 20 | 24 | 11 | 15 | 0 | 1 | 1 | −1 | 1 | 1 | 0 | **3** | 38, 40[a], 41 |
| C28 | Mangbai—Balché 1[d] | 560 | 600 | 359 | 6 | **84** | **204** | 12 | *75* | – | – | 28 | 8 | 0 | 1 | 1 | 0 | 0 | 1 | −1 | **2** | 42 |
| C29 | Mangbai—Balché 2 | 560 | 600 | 217 | −46 | **51** | **68** | 5 | *16* | – | – | 11 | 24 | 0 | 0 | 1 | 0 | 0 | 0 | 0 | **1** | 42 |
| **C30** | **Mangbai and Balché 3** | **560** | **600** | **199** | 48 | **−47** | **349** | **6** | **24** | – | – | **13** | **19** | **1** | **0** | **1** | **0** | **0** | **1** | **1** | **4** | **42** |
| C31 | Mulden Group dc3 | 550 | 560 | 278 | −34 | **12** | **270** | 6 | *24* | 10 | 18 | 18 | 16 | 0 | 1 | 1 | ? | 0 | 1 | 0 | **3** | 38, 40[a], 41 |
| C32 | Nosib Group nq3 | 550 | 746 | 102 | −13 | **9** | **295** | ? | *13* | 7 | 13 | 11 | 13 | 0 | 0 | 0 | 0 | 0 | 1 | 1 | **2** | 38, 40[a], 41 |
| C33 | Chela Gp. remag. | 500 | 746 | 120 | −46 | **18** | **320** | 9 | *36* | 9 | 9 | 41 | 8 | 1 | 0 | 0 | −1 | 0 | 0 | 0 | **0** | 39, 40[a], 41 |
| **C34** | **Hook Intrusives** | 508 | 540 | 300 | 50 | **14** | **337** | | *10* | 36 | 36 | 16 | 32 | 1 | 0 | 0 | 0 | 1 | 0 | 1 | **3** | 43, 44[a] |
| West Africa | | | | | | | | | | | | | | | | | | | | | | |
| W1 | Groupe de Char | 987 | 1051 | 34 | 61 | **54** | **32** | 5 | *23* | 7 | 9 | 160 | 6 | 0 | 0 | 0 | 0 | 1 | 0 | −1 | **0** | 45, 46[c], 47 |
| W2 | Char Group Unit I2 | 966 | 1030 | 334 | −24 | **−49** | **27** | 4 | *52* | 1 | 3 | 63 | 3 | 0 | 1 | 1 | 0 | 1 | 0 | −1 | **2** | 48, 46[c], 47 |
| W3 | Atar Group Unit I9 | 723 | 827 | 125 | −7 | **−34** | **67** | 2 | *15* | 5 | 9 | 20 | 9 | 0 | 0 | 1 | 0 | 1 | 1 | −1 | **2** | 48, 46[c], 47 |
| **W4** | **Adma Diorite** | 590 | 620 | 317 | 79 | **34** | **344** | | *62* | 16 | 17 | 22 | 9 | 1 | 1 | 1 | 0 | 0 | 0 | 0 | **3** | 49 |
| W5 | Tabankort Rhyolite | 580 | 600 | 114 | −70 | **30** | **322** | | *8* | 10 | 12 | – | 7 | 0 | 0 | 0 | 0 | 0 | 0 | 1 | **1** | 49 |
| W6 | Ouarzaate Volcanics | 563 | 593 | – | – | **−30** | **57** | – | – | – | – | – | 17 | 1 | 0 | 0 | 0 | 1 | 0 | −1 | **1** | 50 |
| W7 | Amouslek Tuffs | 563 | 593 | – | – | **−41** | **70** | – | – | – | – | – | 11 | 0 | 1 | 0 | 0 | 1 | 0 | −1 | **1** | 50 |
| W8 | Bou Azzer Andesites | 524 | 544 | – | – | **31** | **57** | 8 | *43* | – | – | 11 | 17 | 0 | 1 | 1 | 0 | 1 | 0 | 0 | **3** | 51 |
| W9 | Bou Azzer combined | 524 | 544 | 52 | 66 | **47** | **42** | 9 | *64* | 10 | 10 | 182 | 7 | 0 | 1 | 0 | ? | 1 | 0 | 0 | **2** | 52 |
| W10 | Serie Lie de Vin | 513 | 600 | 124 | −2 | **29** | **243** | 8? | 8 | 10 | 21 | 8 | 21 | 0 | 0 | 0 | 0 | 1 | 0 | −1 | **0** | 53 |
| W11 | Sidi-Said-Maach. remag. | 501 | 513 | 121 | 20 | **−18** | **55** | 17 | *101* | 3 | 6 | 33 | 6 | 0 | 1 | 1 | ? | 1 | 0 | −1 | **2** | 54 |
| W12 | Sidi-Said-Maachou volc. | 501 | 513 | 300 | −31 | **−14** | **51** | 11 | *66* | 4 | 7 | 70 | 6 | 0 | 1 | 1 | 1 | 1 | 1 | 0 | **5** | 54 |
| W13 | Atar Cliff CO7 & 8 | 488 | 542 | 92 | 14 | **0** | **69** | 3 | *23* | 6 | 12 | 9 | 11 | 0 | 1 | 0 | 0 | 1 | 1 | 1 | **4** | 48 |
| **W14** | **Hasi-Messaud Sediments** | 472 | 501 | 27 | 77 | **53** | **26** | 6 | *30* | 5 | 6 | | 3 | 0 | 1 | 0 | 0 | 1 | 0 | 1 | **3** | 55 |

Table 1 (*Continued*)

| | Craton/belt | Age | | Direction | | Paleomagnetic pole | | | | Precision | | | | Quality index | | | | | | | *Q* | Reference |
|---|---|---|---|---|---|---|---|---|---|---|---|---|---|---|---|---|---|---|---|---|---|---|
| | | Minimum | Maximum | Declination | Inclination | Plat | Plon | *N* | *n* | dp | dm | *K* | A95 | 1 | 2 | 3 | 4 | 5 | 6 | 7 | | |
| Arabia-Nubia | | | | | | | | | | | | | | | | | | | | | | |
| **N1** | **Suakin Gabbro** | 837 | 845 | 244 | −4 | **−25** | **314** | 9 | *49* | 4 | 8 | 59 | 7 | 1 | 1 | 1 | 0 | 0 | 0 | 1 | **4** | 56 |
| N2 | Kadaweb Complex | 713 | 725 | 87 | −24 | **1** | **320** | 2 | *16* | 20 | 20 | 99 | 25 | 0 | 0 | 1 | 0 | 0 | 0 | 1 | **2** | 57 |
| N3 | Chromite Ores | 670 | 900 | 198 | −44 | **74** | **113** | 5 | *26* | 9 | 9 | 55 | 10 | 0 | 1 | 1 | 0 | 0 | 0 | 0 | **2** | 58 |
| **N4** | **Dokhan Volc. Fm. Hard** | 580 | 611 | 194 | 44 | **−36** | **17** | 5 | *25* | 9 | 15 | 41 | 12 | 1 | 1 | 1 | 0 | 0 | ? | 0 | **3** | 59 |
| **N5** | **Dokhan Volcanic Fm.** | 580 | 606 | 178 | 37 | **−43** | **36** | 10 | *49* | 7 | 11 | 33 | 10 | 1 | 1 | 1 | 0 | 1 | ? | 0 | **4** | 60 |
| N6 | Bir Safsaf Dikes[d] | 573 | 599 | 353 | 27 | **80** | **250** | 7 | *23* | 9 | 9 | 9 | 11 | 0 | 0 | 1 | 0 | 1 | 0 | −1 | **1** | **57** |
| N7 | **Nabati Complex** | 569 | 587 | 338 | 37 | **−68** | **134** | 6 | 53 | 19 | 19 | 15 | 18 | 1 | 0 | 1 | 0 | 0 | 0 | 1 | **3** | 57 |
| **N8** | **Sinyai Metadolerite remag.** | **543** | **551** | 241 | 20 | **−29** | **319** | 1 | *42* | 3 | 5 | 20 | 5 | 1 | 1 | 1 | 0 | 1 | 0 | 1 | **5** | 61 |
| **N9** | **Huqf Supergroup** | **544** | **712** | 169 | 28 | **−52** | **74** | 25 | *86* | – | – | 17 | 7 | 0 | 1 | 1 | 1 | 1 | 1 | 1 | **6** | 62 |
| N10 | Mirbat Sandstone | 550 | | 68 | 18 | **−32** | **334** | 2 | *10* | 4 | 8 | 46 | 7 | 0 | 0 | 1 | 0 | 0 | 0 | 1 | **2** | 63 |
| N11 | Abu Durba Sandstones | 513 | 542 | 269 | 60 | **18** | **341** | 2 | *16* | – | – | 44 | 39 | 0 | 0 | 1 | 0 | 1 | 0 | 0 | **2** | 64 |
| **N12** | **Ntonya Ring Structure** | **509** | **535** | 311 | 43 | **28** | **345** | – | *27* | 1 | 2 | 1000 | 2 | 1 | 1 | 1 | 0 | 0 | 0 | 1 | **4** | 65, 66 |
| N13 | Esh EL composite[d] | 488 | 542 | – | – | **89** | **142** | 22 | – | – | – | 101 | 12 | 0 | 1 | 1 | 0 | 0 | 1 | −1 | **2** | 67 |
| N14 | Qena-Safaga Dikes[d] | 480 | 527 | 358 | 45 | **87** | **304** | 25 | *126* | 4 | 6 | 36 | 5 | 1 | 1 | 1 | ? | 0 | 1 | −1 | **3** | 59 |
| N15 | Um Rus Dikes[d] | 480 | 527 | 4 | 39 | **85** | **166** | 14 | *88* | 4 | 7 | 48 | 6 | 1 | 1 | 1 | ? | 0 | 1 | −1 | **3** | 59 |
| N16 | Dokhan Volc, Fm B Remag | 450 | 550 | 318 | 54 | **−54** | **147** | – | *6* | 15 | 22 | 20 | 15 | 0 | 0 | 1 | 0 | 0 | 0 | 0 | **1** | 59 |
| São Francisco[f] | | | | | | | | | | | | | | | | | | | | | | |
| **S1** | **Olivença Dikes R** | 1060 | 1096 | 299 | 61 | **−9** | **323** | 18 | *47* | – | – | 17 | 9 | 1 | 1 | 1 | 0 | 1 | 1 | 1 | **6** | 68 |
| **S2** | **Salvador/Olivença Dikes R** | 1060 | 1096 | – | – | **−9** | **324** | 25 | – | – | – | 21 | 7 | 1 | 1 | 1 | 1 | 0 | 1 | 1 | **6** | 69 |
| **S3** | **Itaju do Colônia Dikes** | 1010 | 1080 | 99 | −72 | **−16** | **343** | 23 | *52* | – | – | 11 | 10 | 0 | 1 | 1 | 0 | 0 | 1 | 1 | **4** | 68 |
| **S4** | **Olivença Dikes N** | 1010 | 1080 | 82 | −71 | **−25** | **345** | 31 | *83* | – | – | 12 | 8 | 0 | 1 | 1 | 0 | 1 | 1 | 1 | **5** | 68 |
| **S5** | **Salvador Dikes R** | 1010 | 1080 | 291 | 65 | **−10** | **328** | 7 | *18* | – | – | 44 | 9 | 0 | 1 | 1 | 1 | 0 | 1 | 1 | **5** | 69 |
| **S6** | **Salvador/Itaju/Olivença N** | 1013 | 1020 | – | – | **−19** | **345** | 62 | – | – | – | 11 | 6 | 1 | 1 | 1 | 1 | 0 | 1 | 1 | **6** | 69 |
| **S7** | **Ilhéus Dikes** | 998 | 1036 | 60 | −67 | **−39** | **352** | 17 | *51* | – | – | 79 | 4 | 1 | 1 | 1 | 0 | 1 | 0 | 1 | **5** | 68 |
| **S8** | **Salvador Dikes N** | 970 | 1036 | 111 | −79 | **−7** | **351** | 8 | *35* | – | – | 15 | 15 | 0 | 1 | 1 | 1 | 0 | 1 | 1 | **5** | 69 |
| S9 | Itabuna Dikes 2 | 762 | 800 | 265 | −16 | **−42** | **266** | 10 | *55* | – | – | 43 | 8 | 0 | 1 | 1 | 0 | 0 | 0 | 0 | **2** | 42 |
| **S10** | **Itabuna Dikes 3** | 762 | 800 | 245 | 54 | **−49** | **337** | 10 | *41* | – | – | 20 | 11 | 0 | 1 | 1 | 0 | 0 | 1 | 0 | **3** | 42 |
| S11 | Itabuna Dikes 1[d] | 646 | 674 | 350 | −26 | **40** | **263** | 13 | *57* | – | – | 51 | 6 | 1 | 1 | 1 | ? | 0 | 0 | −1 | **3** | 42 |
| S12 | Lavras-Pará de Minas Dikes | 550 | 760 | 239 | −18 | **63** | **58** | 16 | *38* | – | – | 19 | 9 | 0 | 0 | 1 | 0 | 1 | 0 | 0 | **2** | 70 |
| **S13** | **Bambuí carbonates B** | 500 | 550 | 26 | 68 | **27** | **359** | 33 | *369* | – | – | 104 | 3 | 0 | 1 | 1 | 0 | 1 | 0 | 0 | **3** | 71 |
| **S14** | **Bambuí carbonates C** | 500 | 550 | 7 | 58 | **32** | **339** | 17 | *116* | – | – | 91 | 4 | 0 | 1 | 1 | 0 | 1 | 0 | 0 | **3** | 71 |
| **S15** | **Salitre Carbonates B** | 500 | 550 | 34 | 61 | **44** | **3** | 13 | *71* | – | – | 17 | 10 | 0 | 1 | 1 | 0 | 1 | 0 | 0 | **3** | 72 |
| **S16** | **Salitre Carbonates C** | 500 | 550 | 6 | 63 | **34** | **339** | 24 | *233* | – | – | 24 | 4 | 0 | 1 | 1 | 0 | 1 | 0 | 0 | **3** | 72 |
| **S17** | **Salitre + Bambuí C** | 500 | 550 | – | – | **34** | **339** | 41 | *349* | – | – | 65 | 3 | 0 | 1 | 1 | 0 | 1 | 0 | 0 | **3** | 72 |
| Amazon[f] | | | | | | | | | | | | | | | | | | | | | | |
| **A1** | **Nova Floresta** | 1195 | 1201 | 294 | −60 | **3** | **34** | 16 | *123* | – | – | – | 6 | 1 | 1 | 1 | 0 | 1 | 0 | 1 | **5** | 73 |
| A2 | Puga cap carbonates A[d] | 580 | 630 | 181 | 39 | **51** | **249** | 13 | *51* | 6 | 9 | – | 8 | 0 | 1 | 1 | 0 | 1 | 1 | −1 | **3** | 74 |
| A3 | Puga cap carbonates B | 520 | 540 | 26 | 55 | **38** | **340** | 16 | *74* | 7 | 10 | – | 7 | 0 | 1 | 1 | −1 | 1 | 0 | 1 | **2** | 74 |
| Rio de Plata – Luíz Alves[f] | | | | | | | | | | | | | | | | | | | | | | |
| **RP1** | **La Tinta Fm.** | 685 | 733 | 360 | −66 | **−48** | **96** | – | *53* | 5 | 5 | 17 | 5 | 1 | 1 | 1 | 0 | 1 | 1 | 1 | **6** | 75 |
| RP2 | Playa Hermosa Fm. | 600 | | 226 | 24 | **−76** | **193** | 2 | *6* | 9 | 16 | 21 | 15 | 0 | 0 | 1 | 0 | 0 | 0 | 1 | **2** | 76 |
| RP3 | Hilário Fm | 591 | 614 | 108 | −4 | **−25** | **272** | 4 | *11* | – | – | 97 | 9 | 1 | 0 | 1 | 0 | 0 | 0 | 1 | **3** | 77 |
| RP4 | Vargas Fm. | 580 | 615 | 110 | 81 | **−17** | **23** | 2 | *7* | – | – | 5 | 30 | 0 | 0 | 1 | 0 | 0 | 0 | 0 | **1** | 77 |

| | | | | | | | | | | | | | | | | | | | | | | |
|---|---|---|---|---|---|---|---|---|---|---|---|---|---|---|---|---|---|---|---|---|---|---|
| RP5 | Acampamento Velho 1 | 567 | 581 | 156 | 69 | **−31** | **51** | 3 | *8* | – | – | 20 | 28 | 0 | 0 | 1 | 0 | 0 | 1 | 0 | **2** | 77 |
| RP6 | Acampamento Velho 2 | 567 | 581 | 207 | −15 | **55** | **340** | 3 | *7* | – | – | 12 | 37 | 0 | 0 | 1 | 0 | 0 | 1 | 0 | **2** | 77 |
| **RP7** | **Sierra de las Animas 2** | 540 | 560 | 95 | −60 | **−47** | **312** | 6 | *27* | 16 | 22 | 22 | 15 | 1 | 1 | 1 | 0 | 1 | 1 | 1 | **6** | 76 |
| **RP8** | **Sierra de las Animas 1** | 501 | 520 | 45 | 58 | **25** | **11** | 7 | *33* | 20 | 27 | 12 | 18 | 0 | 0 | 1 | 0 | 1 | 0 | 1 | **3** | 76 |
| LA1 | Castro Group | 593 | 607 | 347 | −52 | **−38** | **70** | 4 | *20* | – | – | 37 | 15 | 1 | 0 | 1 | 0 | 0 | 0 | 0 | **2** | 77 |
| **LA2** | **Campo Alegre Gp.** | 569 | 627 | 36 | −40 | **−82** | **52** | 6 | *46* | – | – | 56 | 9 | 1 | 1 | 1 | 1 | 0 | 1 | 1 | **6** | 77, 78[a] |
| Brasiliano belts[f] | | | | | | | | | | | | | | | | | | | | | | |
| B1 | Sobral Dikes 1 | 543 | 581 | 26 | 20 | **76** | **294** | 7 | *25* | – | – | 43 | 9 | 1 | 1 | 0 | 0 | 0 | 0 | 0 | **2** | 79 |
| B2 | Sobral Dikes 2 | 543 | 581 | 5 | 78 | **25** | **347** | 1 | *18* | – | – | 10 | 16 | 0 | 0 | 0 | 0 | 0 | 0 | 0 | **0** | 79 |
| B3 | Sobral Dikes 3 | 543 | 581 | 308 | 16 | **0** | **279** | 1 | *11* | – | – | 28 | 9 | 0 | 0 | 0 | 0 | 0 | 0 | 0 | **0** | 79 |
| **B4** | **Itabaiana Dikes** | 520 | 530 | 168 | −64 | **31** | **331** | 15 | *120* | – | – | 28 | 7 | 1 | 1 | 1 | 1 | 1 | 1 | 1 | **7** | 80 |
| B5 | Itaqui Complex 1 | 520 | 670 | 133 | 29 | **4** | **223** | 8 | – | – | – | 15 | 15 | 0 | 1 | 1 | 0 | 0 | 0 | 1 | **3** | 81 |
| B6 | Itaqui Complex 2 | 520 | 670 | 115 | −26 | **−17** | **291** | 9 | – | – | – | 23 | 11 | 0 | 1 | 1 | 0 | 0 | 0 | 1 | **3** | 81 |
| **B7** | **Seridó granites 1** | 520 | 540 | – | – | **13** | **340** | – | – | – | – | 7 | 10 | 0 | 0 | 1 | 0 | 0 | 1 | 1 | **3** | 82 |
| B8 | Seridó granites 2 | 520 | 540 | – | – | **66** | **355** | – | – | – | – | 24 | 7 | 0 | 1 | 1 | 0 | 0 | 1 | 0 | **3** | 82 |
| B9 | Umarizal granitoids | 520 | 554 | 72 | 85 | **14** | **10** | 18 | *62* | – | – | 6 | 16 | 0 | 0 | 1 | 0 | 0 | 0 | 1 | **2** | 82 |
| B10 | Juiz de Fora Complex | 500 | 535 | 3 | 75 | **12** | **358** | 30 | *176* | – | – | 8 | 10 | 0 | 1 | 1 | 0 | 1 | 0 | 0 | **3** | 83 |
| B11 | Piquete complex | 500 | 535 | 60 | 68 | **24** | **23** | 9 | *20* | – | – | 26 | 10 | 0 | 1 | 1 | 0 | 1 | 0 | 0 | **3** | 84 |
| B12 | Tauá Dikes 1[d] | 442 | 615 | 354 | −14 | **44** | **260** | 6 | – | – | – | 72 | 8 | 0 | 1 | 1 | 0 | 0 | 0 | −1 | **1** | 42 |
| B13 | Tauá Dikes 2 | 442 | 615 | 47 | 17 | **80** | **61** | 5 | – | – | – | 32 | 14 | 0 | 0 | 1 | 0 | 0 | 1 | 0 | **2** | 42 |
| B14 | Tauá Dikes 3 | 442 | 615 | 144 | 57 | **−10** | **53** | 5 | – | – | – | 24 | 19 | 0 | 0 | 1 | 0 | 0 | 0 | 0 | **1** | 42 |

Boldface poles are used in the construction of Apparent Polar Wander Paths (APWPs). *N*, number of sites; *n*, number of demagnetized samples used to calculate paleomagnetic pole; *Q* index criteria (1–7) are summarized as follows: (1) good age constraints for the magnetization, (2) statistical precision (A95 < 16°) from adequate sample number (>24) gathered from large geographic area, (3) detailed demagnetization illustrated via vector subtraction, (4) field tests for timing of magnetization, (5) structural control/continuity with the craton, (6) presence of reversals, and (7) dissimilarity from more recent paleomagnetic directions. (1) Briden et al. (1979); (2) Renne et al. (1990); (3) Jones (1968); (4) Doppelhammer and Hargraves (1994); (5) Ito et al. (1978); (6) Onstott and Hargraves, 1981; (7) Powell et al. (2001); (8) Piper (1975); (9) Hoal and Heaman (1995); (10) Hanson et al. (1998); (11) McElhinny and Opdyke (1964); (12) Jones and McElhinny (1966); (13) Allsop et al. (1986); (14) Hargraves et al. (1994); (15) Hanson et al. (2004); (16) McElhinny (1966); (17) Mare and Thomas (1997); (18) Jacobs et al. (1997); (19) Gose et al. (2004); (20) Onstott et al. (1986a); (21) Gutzmer et al. (2000); (22) Kröner et al. (1980); (23) Saylor et al. (1995); (24) Grotzinger et al. (1995); (25) Reid et al. (1991); (26) Onstott et al. (1986b); (27) Meert et al. (1997); (28) Reid (1968); (29) Brock et al. (1972); (30) Pinna et al. (2000); (31) Piper (1974); (32) Deblond et al. (2001); (33) Piper (1972); (34) Carvalho et al. (2000) (see also Mayer et al., 2000); (35) Meert et al. (1994); (36) D'Agrella-Filho et al. (1996); (37) Meert et al. (1995); (38) McWilliams and Kröner (1981); (39) Jones et al. (1992); (40) Hoffman et al. (1996); (41) Hoffmann et al. (2004); (42) Ponte (2001); (43) Brock (1967); (44) Hanson et al. (1993); (45) Morris and Carmichael (1978); (46) Kent et al. (1984); (47) Perrin and Prévot (1988); (48) Perrin et al. (1988); (49) Morel (1981); (50) Hailwood and Tarling (1973); (51) Hailwood (1972); (52) Daly and Pozzi (1977); (53) Martin et al. (1978); (54) Khattach et al. (1995); (55) Bucur (1971); (56) Reischmann et al. (1992); (57) Saradeth et al. (1989); (58) Refai et al. (1989); (59) Davies et al. (1980); (60) Nairn et al. (1987); (61) Meert and Van der Voo (1996); (62) Kilner et al. (2005); (63) Kempf et al. (2000); (64) Abdeldayem et al. (1994); (65) Briden (1968); (66) Briden et al. (1993); (67) Van der Voo and Meert (1991); (68) D'Agrella-Filho et al. (1990); (69) D'Agrella-Filho et al. (2004a); (70) D'Agrella-Filho (1992); (71) D'Agrella-Filho et al. (2000); (72) Trindade et al. (2004); (73) Tohver et al. (2002); (74) Trindade et al. (2003); (75) Valencio et al. (1980); (76) Sánchez-Bettucio and Rapalini (2002); (77) D'Agrella-Filho and Pacca (1988); (78) Citroni et al. (2001); (79) Guerreiro and Sial (1982); (80) Trindade et al. (2006) (submitted to Earth and Planetary Science Letters); (81) Correia and Ernesto (1998); (82) Trindade (1999); (83) D'Agrella-Filho et al. (2004b); (84) D'Agrella-Filho et al. (1986).

[a] Superseding geochronological reference number, where not included in the referenced paleomagnetic study.

[b] Contact test inferred from Jones and McElhinny (1966) and Mushayandebvu et al. (1994).

[c] Magnetic component, originally considered as primary, reported to be of probable secondary origin by reference #.

[d] PDF—possible overprint by present-day field.

[e] Paleomagnetic poles no longer considered as belonging to 1200–500 Ma studied interval based on new geochronological data.

[f] Position of paleomagnetic poles depicted in African coordinates using the using Euler pole [45.5N, −32.2E, +58.2] from Lawver and Scotese (1987).

zation demonstrating the isolation of the characteristic magnetization through vector subtraction, (4) field tests that clarify the timing of magnetization, (5) structural continuity of the studied region with the craton it represents, (6) presence of reversals, and (7) demonstrated distinctiveness of the reported paleomagnetic direction from more recent magnetic overprints. Reported results that fail one of these criteria are indicated with a minus (−1) sign in Table 1 and a reference to any repudiating study is provided in Table 1. This modification in the application of Van der Voo's (1990) *Q*-analysis calls attention to results that are based on suspected remagnetizations (where a failed field test is available) or in cases where the reported paleomagnetic direction bears a clear resemblance to a younger direction of known age. Results based on directions that lie close to the mod-

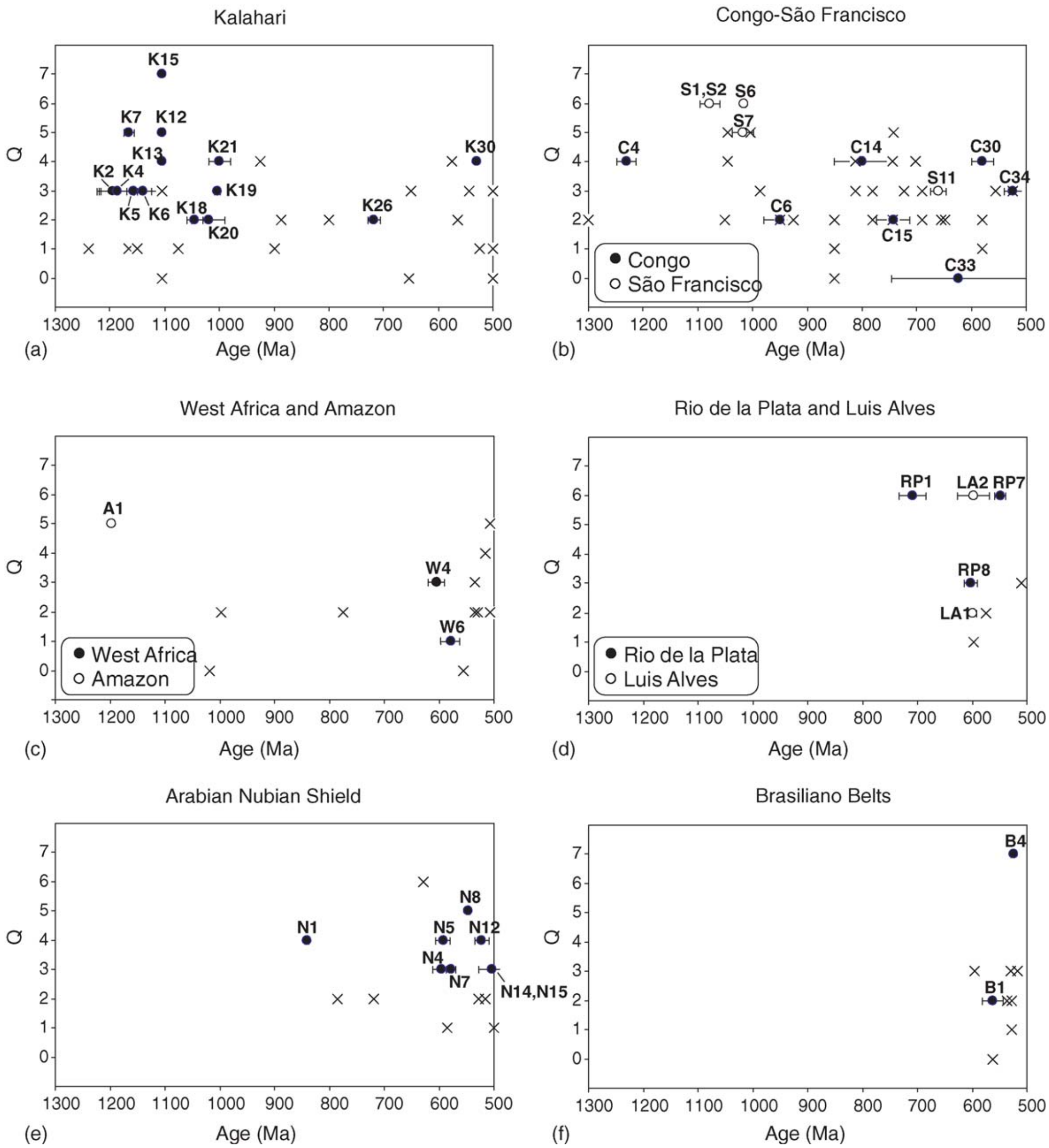


Fig. 2. Plot of the age distribution of individual paleomagnetic poles versus the reliability index (*Q*, of Van der Voo, 1990) for west Gondwanan cratons and shield areas. Paleomagnetic poles with an established age (usually a radiogenic isotope age with an error margin of ±4%) are depicted with circles and age error bars. Other poles with less well-established (e.g. geological constraints or regional correlation) are represented by X's over an inferred age range.

ern field direction are also indicated in the table, with the caveat that these results may well reflect an ancient field with a direction treacherously close to the modern field. Only further work will confirm the validity of these suspect results. In theory, a remagnetization of *known* age is as useful for paleogeography as a primary result. Unfortunately, the many and lengthy gaps in the West Gondwanan drift record leave considerable uncertainty as far as recognizing and assigning an age to such remagnetizations.

The availability of paleomagnetic data from each of the studied cratons is not uniform in quality nor are all time intervals equally represented, as indicated by the plot of $Q$ index versus pole age for each of the cratons (Fig. 2). Only those poles whose age is known to within ±4% (error bars in Fig. 2) are used for paleogeographic purposes, thus satisfying the most critical factor of the $Q$ index. Most poles, however, have low $Q$ values and very poor age constraints. Of the 148 poles considered here, only nine were graded with $Q$ values of 6 or higher, meaning that significant portions of the continents' drift history should be regarded with skepticism. Consequently, only limited portions of the apparent polar wander (APW) paths can be traced for most of the considered cratonic units in Figs. 3–7. With the exception of the Kalahari and São Francisco–Congo cratons, the number of available paleomagnetic poles increases for times after 650 Ma, an interval marked by extensive tectonic

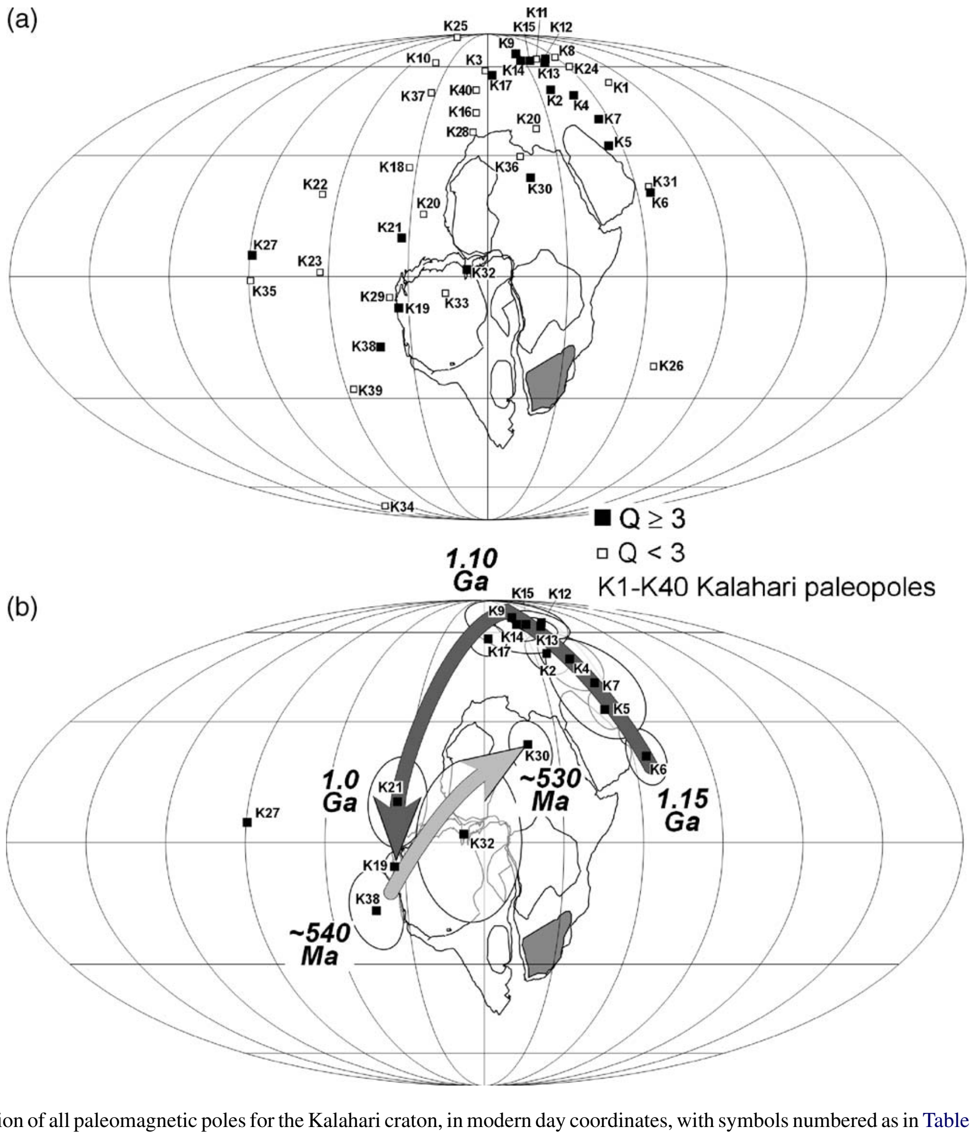


Fig. 3. (a) Position of all paleomagnetic poles for the Kalahari craton, in modern day coordinates, with symbols numbered as in Table 1. (b) Relatively continuous segments of apparent polar wander are shown by different colored arrows, as discussed in text. Black symbols with $Q \geq 3$ that are not used in construction of APWP are shown without confidence circles.

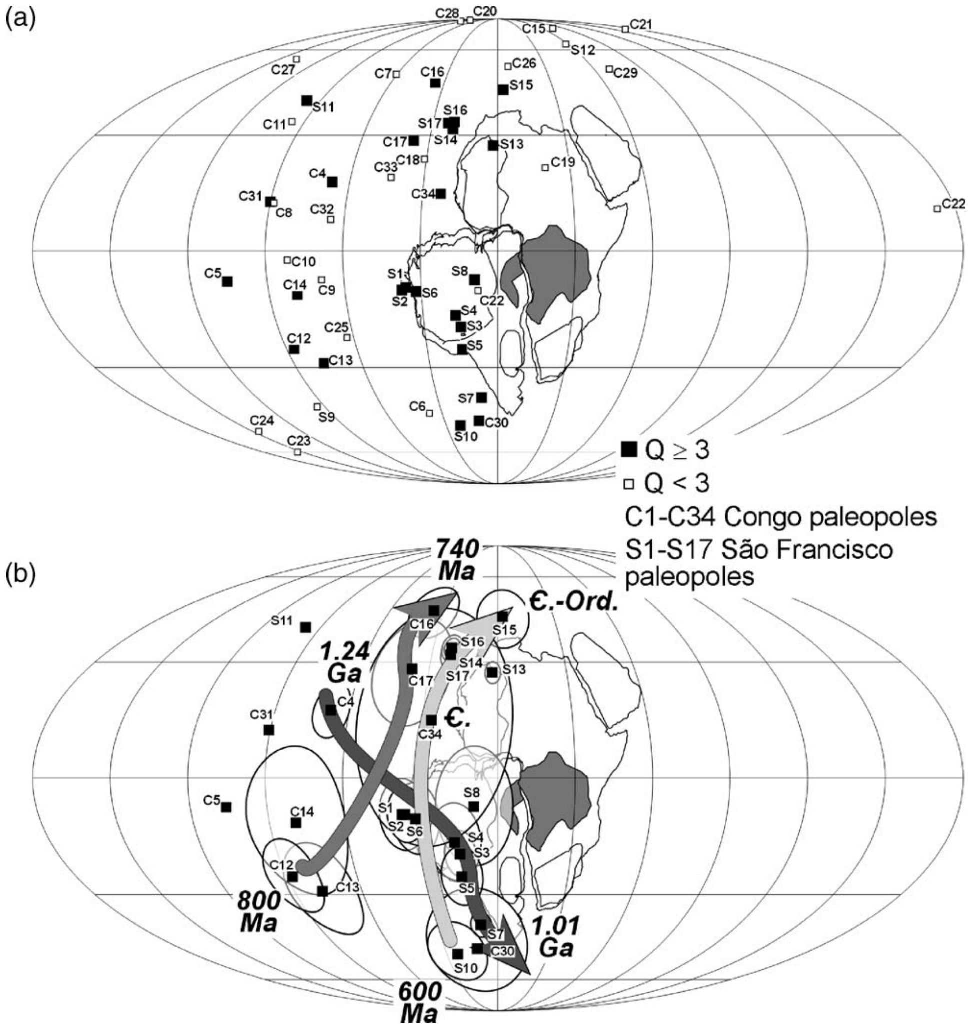


Fig. 4. (a) Position of all paleomagnetic poles for the Congo craton, in modern day coordinates, with symbols numbered as in Table 1. (b) As for Fig. 3b.

activity related to the Panafrican/Brasiliano orogenies that record the assembly of Gondwana. Although unambiguous tests of Rodinia paleogeography throughout the duration of this supercontinent are not possible, given the uneven data coverage, a broad outline of the transition from Rodinia to Gondwana can be reconstructed from the present data. In the discussion that follows, we provide a summary of paleomagnetic data we believe to be reliable for each tectonic unit in light of the *Q*-factor analysis, as well as the results from recent studies.

### 2.1. Kalahari

The Kalahari craton is the best studied of all the African cratons, having benefited from paleomagnetic investigations beginning in the 1960's. The results accumulated over this long period are of mixed quality (Fig. 2a) with widely dispersed paleopole positions reported even for relatively short intervals (Fig. 3a). The best results for the Kalahari craton are from the 1200–1000 Ma interval. They are grouped chronologically into four distinct clusters of poles, based on both geochronology and paleomagnetic directions, with a well-defined APW path only for the interval between ca. 1160 and 1000 Ma (Fig. 3a).

The oldest results for the considered time interval come from numerous studies of late Mesoproterozoic kimberlites, with most ages in the 1200–1150 Ma range (Jones, 1968; Ito et al., 1978; Doppelhammer and Hargraves, 1994). The scatter in paleomagnetic direction (poles K2–K8; Fig. 3a) and the lack of precision in these age determinations (chiefly Rb–Sr and U–Pb whole

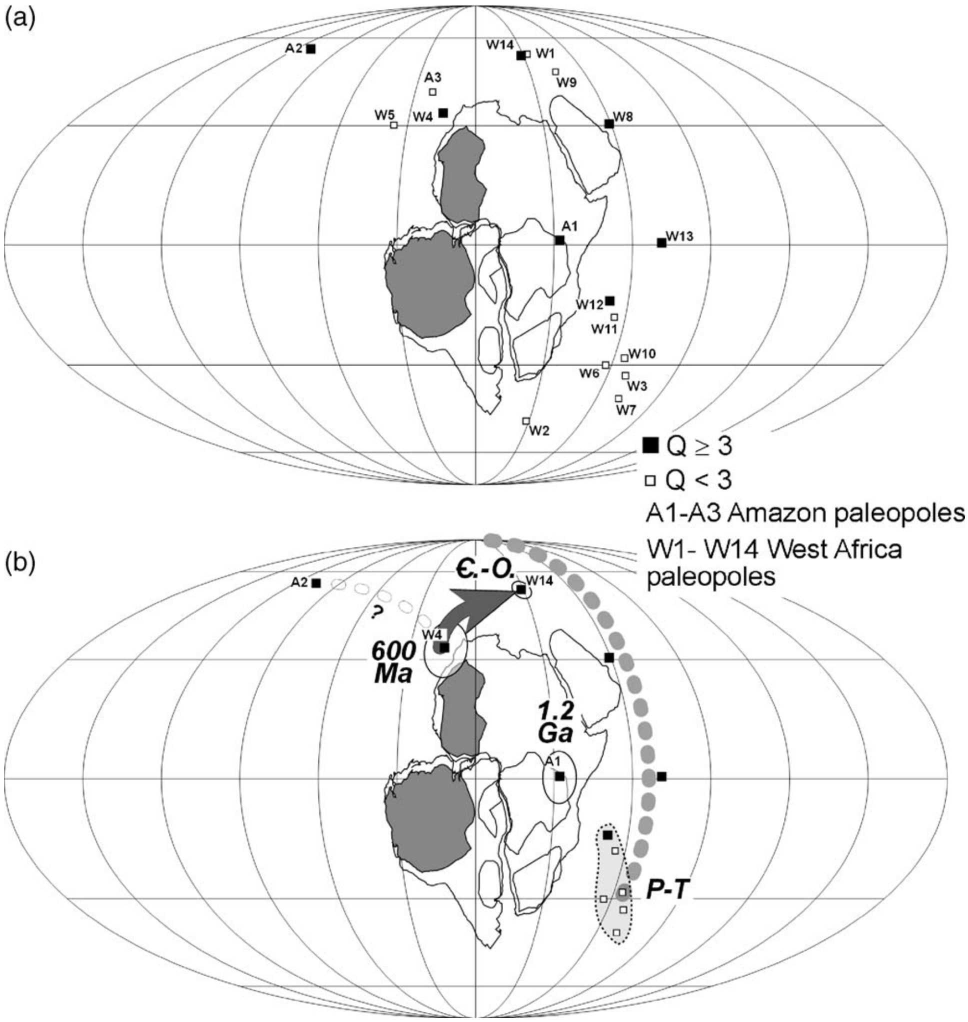


Fig. 5. (a) Position of all paleomagnetic poles for the West Africa-Amazon craton, in modern day West African coordinates using Euler pole [45.5N, −32.2E, +58.2] from Lawver and Scotese (1987), with symbols numbered as in Table 1. (b) As for Fig. 3b. The 630–600 Ma portion of the APW is shown with a dashed line, indicating the uncertainty regarding the primary nature of the Puga A pole (A2). The region enclosed with a dashed line and labeled "P–T" contains poles that appear to be the product of a Permo–Triassic remagnetization acquired during the collision of Gondwana with Laurussia. The remagnetizing effects of this collision are expected to be most pronounced for those results that derive from the northern margin of West Africa. Note that poles W8 and W13 lie along an arced line between the present-day field and the locus of P-T remagnetization, suggesting that they may reflect a mixture of the modern field with a late Paleozoic overprint.

rock data) may reflect faulty age determinations, or the acquisition of magnetization during separate episodes of kimberlite emplacement, or some combination of both factors. Given the difficulties in determining the precise age of kimberlite emplacement (and of magnetic acquisition), we embrace the approach taken by Powell et al. (2001), who calculate an average pole for all reported results, for which an average age of $1165 \pm 10$ Ma is assigned (pole K7 in Table 1 and Fig. 3a). We note that the paleomagnetic directions reported from kimberlites are different from known Phanerozoic directions, suggesting that these results are primary in spite of their low precision.

The second cluster of results derives from the regionally extensive rock units of the ca. 1100 Ma Umkondo intrusive province (Umkondo Lavas and dolerites, Post-Waterberg Diabases, Timbavati Gabbros; poles K12–K15). Consistent paleomagnetic directions measured from cogenetic intrusive and extrusive rocks (e.g. McElhinny, 1966; Hargraves et al., 1994; Hanson et al., 2004) reinforce observations of sequential magnetic reversals (Jones and McElhinny, 1966; Hanson

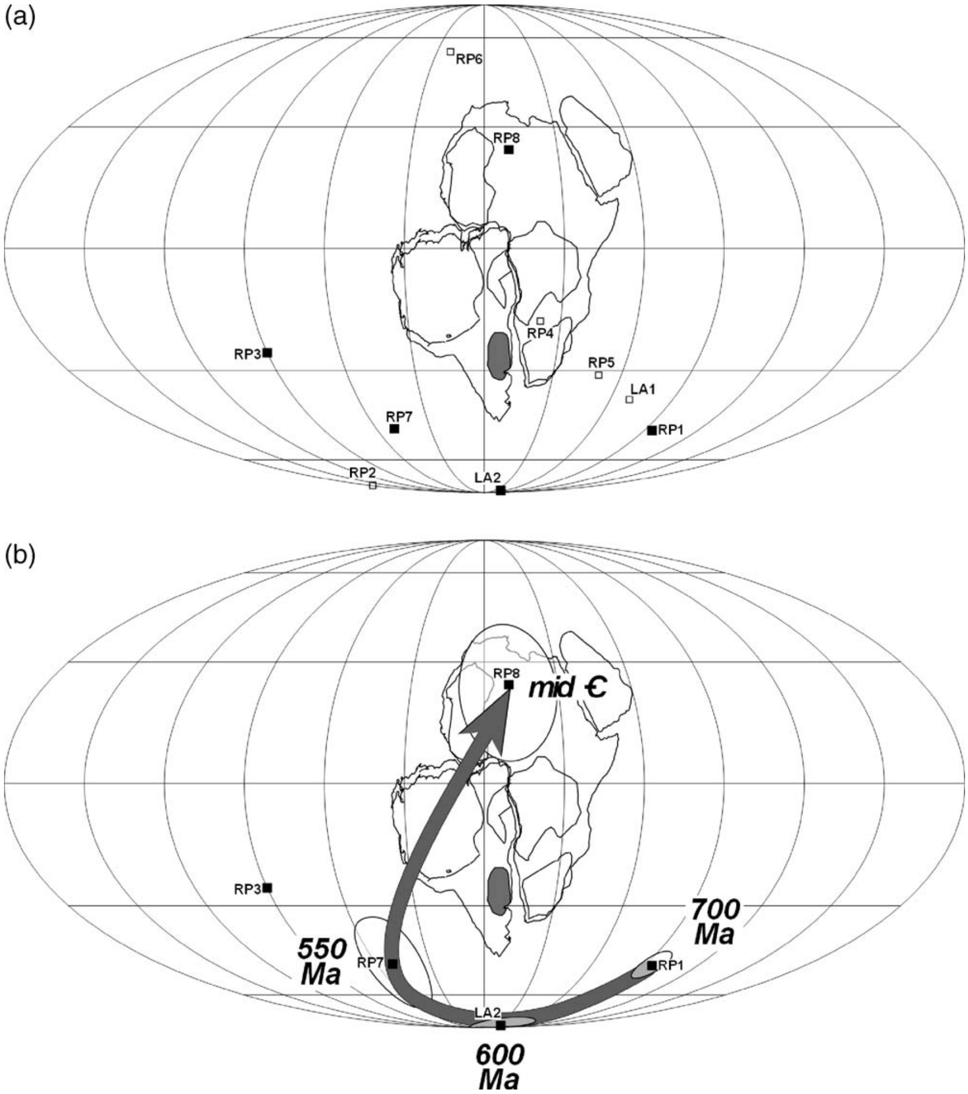


Fig. 6. (a) Position of Rio de Plata/Luiz Alves paleomagnetic poles, shown in African coordinates using Euler pole [45.5N, −32.2E, +58.2] from Lawver and Scotese (1987). (b) As for Fig. 3b.

et al., 2004) and a positive baked contact test (Jones and McElhinny, 1966). The effects of the Umkondo igneous event are also recorded in both the older, crystalline basement rocks (Mushayandebvu et al., 1994) and pre-Umkondo volcanosedimentary formations of the Sinclair Group (>1216 Ma, zircon age from intrusive granite; Hoal and Heaman, 1995). Mafic lavas of these pre-Umkondo rocks, such as the Barby Fm. and Guperas Fm. (K9–K10) studied by Piper (1975), record secondary paleomagnetic directions that reflect the effects of widespread metamorphism and consequent remagnetization and perturbation of the Rb–Sr system, as noted by Onstott et al. (1986a), who attributed the remagnetization to the younger, 1050 Ma Namaquan metamorphic episode. Additionally, a stable magnetic component isolated from the Fe–Mn ore samples of the Kalahari Manganese Field is similar to the characteristic Umkondo direction, suggesting that these Paleoproterozoic rocks were also remagnetized at this time (Evans et al., 2001). Fortunately, the paleomagnetic investigation of the rocks of the Umkondo province has been accompanied by increasingly precise geochronological work, with detailed stacking of magnetic polarity intervals recently refined by SHRIMP analysis (Wingate, 2001; Hanson et al., 2004) resulting in a very robust paleomagnetic record (K15 with $Q = 7$).

A third temporal and spatial cluster of paleomagnetic results derives from studies of the mostly unde-

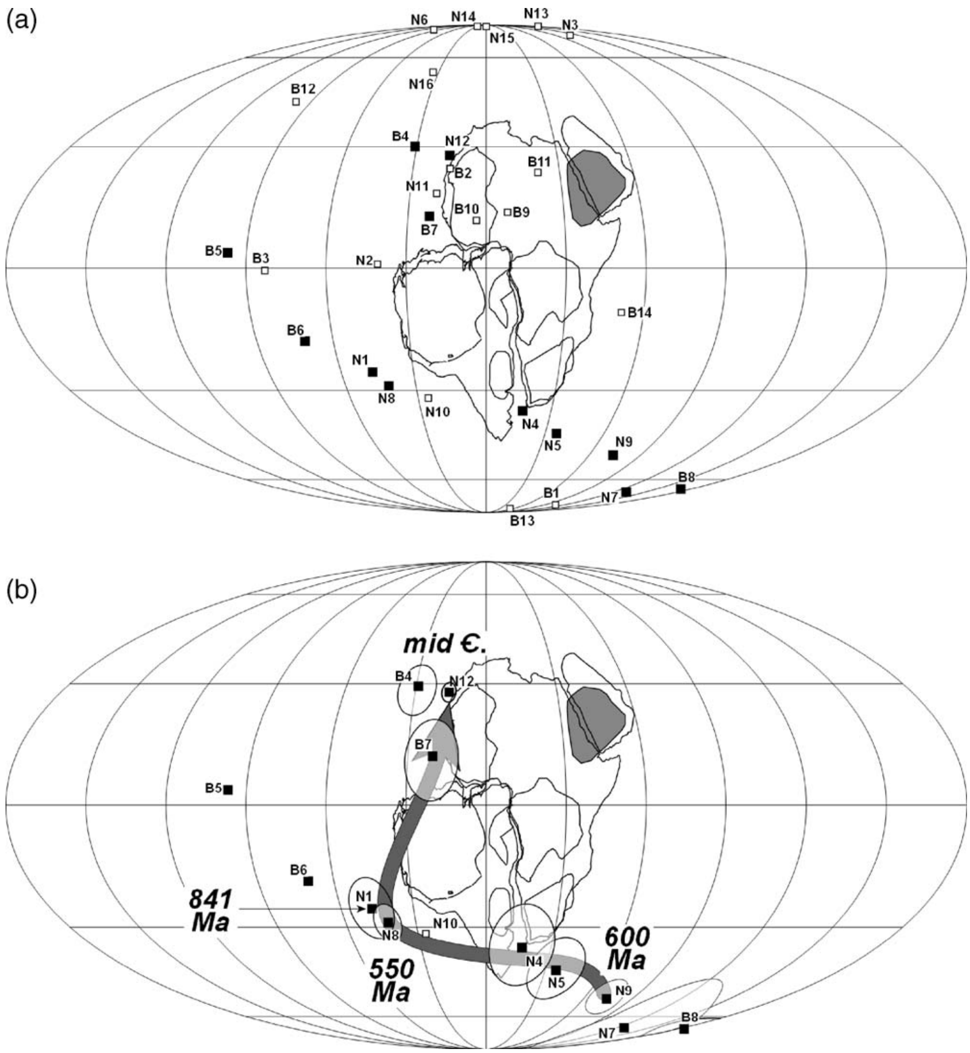


Fig. 7. Position of paleomagnetic poles from Brasiliano belts and the Arabian–Nubian shield, plotted in African coordinates using Euler pole [45.5N, −32.2E, +58.2] from Lawver and Scotese (1987). (b) As for Fig. 3b.

formed, slightly metamorphosed sediments overlying the Sinclair Group (Gutzmer et al., 2000). The Kalkpunt redbeds of the Koras Group and the Auborus Formation (K16–K17) (Piper, 1975), which were correlated by Briden et al. (1979), both yield SSE declinations with low inclinations. Correction for minor tilting of Kalkpunt beds does increase the clustering of paleomagnetic directions, although the difference is too slight to constitute a positive fold test. In the absence of further information to the contrary, we suggest that the Kalkpunt result may be a primary, detrital remanence. The maximum age of these sedimentary sequences is constrained by the presence of an 1170 Ma zircon in the underlying Swartkopsleegte quartz porphyry (SHRIMP analysis; Gutzmer et al., 2000). If these sediments do predate the main thermal episode of Namaquan metamorphism, as suggested by Gutzmer et al. (2000), the ca. 1050 Ma age of this metamorphism may serve as a minimum age limit for the magnetization. The contention that these sequences preserve a primary magnetic direction is supported by the position of the derived paleomagnetic poles between the primary poles of the Umkondo results and the younger poles obtained from the slowly-cooled metamorphic rocks of the Namaqua belt (cluster four, discussed below). This interpretation requires that the deposition of the Koras Gp. (and acquisition of a primary, detrital remanence) occurred after the Umkondo episode and before Namaquan metamorphism.

The fourth group of Kalahari results derives from paleomagnetic study of the high grade rocks of the

Grenville-aged Namaqua-Natal mobile belt, the magnetizations of which have long been interpreted as acquired during slowing cooling in the wake of metamorphism (Onstott et al., 1986a; Renne et al., 1990; Mare and Thomas, 1997; Gose et al., 2004). Assigning precise ages to the resulting paleomagnetic poles (O'Okiep basic intrusives, Port Edward charnockite, Ntimbankulu pluton; poles K18–K20) has proven difficult however, replicating the debate over the age progression of poles from metamorphic rocks of the Grenville belt proper (cf. Costanzo-Alvarez and Dunlop, 1998; Weil et al., 1998; Yu and Dunlop, 2002). Renne et al. (1990) (K21) assigned an age of 1000 ± 20 Ma for the paleomagnetic pole previously reported by Onstott et al. (1986a) by $^{40}Ar/^{39}Ar$ analysis of hornblende and biotite separated from the studied rocks. A similar approach was taken by Mare and Thomas (1997) who included Rb–Sr regional data into their mean, yielding a less precisely dated pole (∼1050 Ma) that is indistinguishable from the Renne et al. (1990) pole. A recent study of the Port Edward Charnockite by Gose et al. (2004) confirms the general paleomagnetic directions discovered by Onstott et al. (1986a), with the acquisition of the magnetization now constrained by additional $^{40}Ar/^{39}Ar$ age dating to 1004 ± 5 Ma (Jacobs et al., 1997).

The certainty of the Kalahari drift history deteriorates substantially after the Namaquan episode. Notably, of the few poles reported for the 900–500 Ma interval (Fig. 3b), many are based on study of assorted pre- to post-tectonic, mafic dikes that intrude the metamorphosed basement rocks. Paleomagnetic poles calculated from these dikes (Pre-Nama dikes, Klein Karas dikes, Gannakouriep dikes; poles K22, K25, K26) are hampered by poorly documented paleomagnetic directions based on a small number of sites and samples, as well as the problem of imprecise dating. (The different names assigned to these rocks masks the fact that all three dike sets may be part of a single episode of mafic dike emplacement; R. Hanson, personal communication.) In other cases, there is also a lack of a discernible directional grouping other than that of the present-day field (e.g. pre-Nama dikes; pole K25). The uncertainty of the post-Namaquan interval is not much improved by study of the late Neoproterozoic stratigraphic sequences. Meert et al. (1997) demonstrated that most of the Nama Group directions previously reported as primary by Kröner et al. (1980) are the result of secondary overprints, most significantly for the "ancient" LN1 pole (K24). Likewise, original work by Piper (1975) indicates a negative fold test for the Doornport Formation (K31), considered to be older than the Nama Gp. (R. Hanson, personal communication). A possible survivor of this widespread remagnetization event is the N5 composite pole (K39) reported by Meert et al. (1997), with a maximum age of 539.4 ± 1 Ma, based on U–Pb zircon analysis for an underlying ash bed (Saylor et al., 1995; Grotzinger et al., 1995). However, a new ∼530 Ma pole from cooled metamorphic rocks (Mzumbe gneiss and Equeefa dikes-K30) reported by Gose et al. (2004) plots close to modern Egypt, a ∼60° difference from the position of pole K39. The ∼10 Ma difference in age inferred for these two poles suggests rapid continental motion in the early Cambrian or problems in the assignment of magnetization age for one of these two poles. Further insight into the true nature and timing of this period of rapid drift may be gained by revisiting the Sijarira Gp. of Zimbabwe, first studied by Reid (1968). The pole (K32) reported from these rocks is flawed by poor age controls and an imprecise paleomagnetic direction. However, the paleopole position between the Nama composite pole (K39) and the Equeefa dikes/Mzumbe gneiss (K30) suggests that these rocks may be of interest to future workers seeking to refine the earliest Cambrian drift history for the Kalahari craton.

### 2.2. *Congo and São Francisco*

Examination of the joint paleomagnetic results from the Congo São Francisco craton is based on the inferred common history between these cratons throughout the Mesoproterozoic. The land bridge between these two Archean-cored blocks is commonly depicted with the narrow basin of the Adamastor Ocean widening to the present-day south, a scenario which is supported by the restriction of the Panafrican/Brasiliano belts (Araçuaí, Ribeira/Mantiqueira, West Congo belts of Fig. 1) to the region south of the land bridge. Evidence of remobilization and thermal resetting in the vicinity of the bridge is entirely absent (Torquato and Cordani, 1981). The joint paleomagnetic record of the São Francisco–Congo craton has paleomagnetic poles from some portion of the entire interval considered here, with three well-defined clusters (Fig. 2b).

The oldest paleomagnetic pole that we consider here is derived from the characteristic magnetic remanence preserved in the post-Kibaran, mafic intrusives of the Mukanda-Buhoro massif (C4), which outcrops in the southern Congo craton (Burundi and Tanzania). Cooling of these rocks through the Curie temperature of magnetite, the principal magnetic carrier, is dated at ca. 1223 Ma by interpolation of U–Pb zircon ages and $^{40}Ar/^{39}Ar$ biotite ages (Meert et al., 1994). This age assignment has been called into question by recent SHRIMP results from these rocks, which suggest an older emplacement age of 1.37 Ga, or the more innocuous possibility of inherited grains (Tahon et al., 2004). A younger group of poles corresponds to the record of 1080–1010 mafic dikes (poles S1–S6) that intrude the basement rocks of the São Francisco craton, in eastern Brazil (D'Agrella-Filho et al., 1990; D'Agrella-Filho et al., 2004b). This set includes two high-quality ($Q = 6$) composite poles (S2 and S6) calculated from normal and reversed components of a similar direction that were obtained from four sets of dikes dated by $^{40}Ar/^{39}Ar$ dating. This age analysis of the paleomagnetic sample material yields ages of 1078 ± 18 Ma (S2) and 1021 ± 8 Ma (S6) for these two poles. Together with the pole for Ilhéus dikes (S7) dated at 1012 ± 24 Ma, they define a well-constrained APW path between 1080 and 1010 Ma (Fig. 4a). Tracing back to the 1223 Ma post-Kibaran intrusions (C4) paleopole forms a continuous, late Mesoproterozoic APW swath for the São Francisco–Congo craton (Fig. 4a) for 1223–1010 Ma. This relatively straight APW path may be marked by a cusp at 950 Ma, as proposed by Weil et al. (1998) on the basis of the location of the ca. 950 Ma Nyabikere massif (C6) virtual geomagnetic pole (VGP). Although the Nyabikere massif VGP position between the 1080 and 1010 Ma and the next youngest cluster of ca. 800 Ma poles suggests that it may indeed record the paleogeographic position of the Congo craton at 950 Ma, there is reason to doubt the validity of this pole (Meert and Torsvik, 2003). Given the very small number of samples (four samples from a single site) used in the original study, and the fact that the remanence in these samples was acquired at an uncertain time in the wake of high grade metamorphism, we choose not to include the Nyabikere result in determining the drift history of the São Francicso–Congo craton (Fig. 4b). We also forebear from including the Gabon dikes pole (C5) reported by D'Agrella-Filho et al., 1996, simply noting that the position of this pole may be evidence of a loop in the APWP proposed by other workers (e.g. Weil et al., 1998). At present, geochronological controls for these rocks are poor, established by correlation with well-dated equivalents in the São Francisco craton (D'Agrella-Filho et al., 2004b).

Following the well-defined 1220–1010 Ma portion of the APWP, a younger cluster of Neoproterozoic poles is centered about the Gagwe lavas (C12, C13) and associated Bukoban intrusives (C14) (Fig. 4b) that were first studied by Piper (1972) with refined paleomagnetic directions presented by Meert et al. (1995). Recent $^{40}Ar/^{39}Ar$ geochronological data demonstrates the age of Gagwe lavas to be 795 ± 7 Ma (Deblond et al., 2001) emplaced while the SFC was at very low latitudes, as indicated by the shallow inclination of the paleomagnetic direction. A high-quality paleomagnetic result from the ca. 743 Ma Mbozi complex (C16) also demonstrates a low latitude position. The position of this younger pole relative to the SFC indicates that the craton drifted across the equator from 795 to 743 Ma, rotating by approximately 90° in the process. This conclusion is corroborated by preliminary paleomagnetic data from the 765 Ma Luakela basalts and basaltic-andesites of Zambia (Wingate et al., 2004, pole not reported), for which a dual polarity, high temperature remanence has been isolated. Accepting both the Gagwe and Mbozi results as valid requires a 90° rotation of the São Francisco–Congo craton in an interval of no <60 Ma, with even faster rotation rates inferred from the Luakele result (assuming that the 795 Ma Gagwe result is not a younger remagnetization). Future work will doubtlessly shed light on this period of apparently rapid drift rates: one possible avenue for future work is revisiting some of the rock units first studied by Piper (1972, 1974). Intriguingly, paleomagnetic results from the Neoproterozoic Kigonero Flags (C8), Malagarasi Sandstone (C9), and Mbala Dolerites (C10), though too imprecise from both the paleomagnetic (small sample size) and geochronological standpoint to be included in an APWP, indicate paleopole positions between the Gagwe and Mbozi/Luakela poles.

Paleomagnetic results from the ca. 743 Ma volcanic rocks described above are concordant with directions isolated from the sedimentary rocks of the Nosib Gp. U–Pb zircon ages obtained from volcanic rocks of the uppermost Nosib Gp. (Hoffman et al., 1996) and interbedded with the overlying Otavi Gp. (Hoffmann et al., 2004) provide much better geochronological constraints than were available at the time of the original paleomagnetic study (McWilliams and Kröner, 1981), and indicate that the deposition of the Nosib Gp. and the cooling of the Mbozi complex were penecontemporaneous. A positive fold test for the oldest magnetic component from the Nosib Gp. rocks (NQ1-high temperature; pole C17) is obtained by comparison with a high temperature component isolated from samples of the time-equivalent Chela Gp. rocks (C18) of Angola (Jones et al., 1992), which are correlated to the Nosib Gp. rocks (Kröner and Correia, 1980). Thus, the 744 ± 2 Ma zircon age of Hoffman et al. (1996) provides an approximate (minimum?) age for a paleomagnetic pole that falls between the ca. 800 Ma results from the Gagwe lavas and Bukoban intrusives and the 743 Ma results from the Mbozi complex. The APWP segment between poles C12 and C16 is indicated in Fig. 4b.

For Precambrian times younger than ca. 740 Ma, there are few well-dated paleomagnetic results, with the exception of two poles recently obtained by Ponte-Neto (2001) for the Mangbai and Balché massifs of Cameroon and the Itabuna dikes pole from the São Francisco craton (poles C30 and S10) (Fig. 4a and b), both of which yield three magnetic components. A present-day field overprint is common to both sets of studied samples; calculated poles from this possible overprint (S11, C28) are barred from further consideration. For the remaining two magnetic directions from both studied regions, we discard the intermediate component 2 as being of questionable significance. The remaining high coercivity, high-temperature components from the Mangbai-Balché massifs (C30) and the Itabuna dikes (S10) are interpreted as primary. Both sets of studied samples yield poles located off the southwestern coast of present-day Africa (C30). The 580 ± 20 Ma age of the C30 pole is based on an Rb–Sr isochron obtained on the same samples collected for paleomagnetic study (Montes-Lauar et al., 1997).

A younger, well-defined group of poles (Fig. 4b) corresponds to the results obtained on Neoproterozoic marine carbonates found on the São Francisco craton (Bambui Group and Salitre Formation) first studied by D'Agrella-Filho et al. (2000). Subsequent paleomagnetic, rock magnetic, and Pb isotopic studies on these rocks demonstrate the ubiquitous effects of remagnetization together with resetting of the U–Pb isotopic system at about 530–520 Ma ago (Trindade et al., 2004). The corresponding paleomagnetic poles (S13, S14, S15, S16, and the composite pole S17) define the Cambrian segment of the São Francisco–Congo APW path, and partially coincide with other secondary remagnetizations reported from the Nosib Gp. (C32) and correlated Chela volcanoclastics (C33), studied by McWilliams and Kröner (1981) and Jones et al. (1992), respectively. A paleomagnetic pole (C34) from the well-dated Hook Intrusives (U–Pb zircon; Hanson et al., 1993), though marred by high degree of directional uncertainty ($\alpha_{95} = 32°$), provides a geochronological anchor for the Cambrian age of the above remagnetizations. Thus, there is clear evidence for a mid-Cambrian (520–530 Ma) paleomagnetic pole position for the São Francisco–Congo just off the northwestern Atlantic coast of Africa, in the vicinity of modern-day Morocco to Mauritania (Fig. 4b).

### 2.3. Amazon and West Africa

The West African and Amazon cratons have the most poorly constrained drift histories during the studied interval of any of the major cratons, with only one well dated pole per unit (Fig. 2c). Beginning our discussion with West Africa, we note that virtually all of the published poles for this craton come from investigations of fossil-free Precambrian sedimentary rocks that are difficult to date directly, absent interbedded volcanic layers. Many of these sequences were remagnetized during the late Paleozoic assembly of Pangea (Kent et al., 1984; Perrin and Prévot, 1988; Perrin, 1994; Weil et al., 2001). For example, the Char and Atar Groups (poles W1–W3) have ages of ca. 1000 and 775 Ma as determined by Rb–Sr dating of diagenetic clays, and would appear to be ideal for the post-Grenville, pre-Iapetan time interval. However, the paleomagnetic directions preserved in these rocks either overlap perfectly with the SE, shallow directions expected for the late Paleozoic (Kent et al., 1984; Perrin and Prévot, 1988) or suggest intermediate mixtures of the late Paleozoic direction with the modern field (Perrin, 1994). Similar paleomagnetic results are obtained from the late-Neoprotoreozoic to Cambrian rocks (e.g. Daly and Pozzi, 1977; Martin et al., 1978; Morris and Carmichael, 1978; Kent et al., 1984; Perrin and Prévot, 1988; Perrin et al., 1988; Perrin, 1994; Khattach et al., 1995) found throughout West Africa (Moussine-Pouchkine and Bertrand-Sarfati, 1997). The suspect region for paleomagnetic poles calculated from mixed secondary directions of the late Paleozoic overprint ("P–T" area enclosed with dashed line) and the modern day field is shown by the grey, dotted line in Fig. 5b, which clearly overlaps most of the reported West African results (W2–W3; W6–W8, W10–W13). These results are excluded from further consideration in the construction of an APW path. Of these excluded results, the Sidi-Saïd-Maâchou pole (W12), of alleged mid-Cambrian age, bears further discussion because of the positive fold test reported for the high temperature magnetic component isolated in these rocks (Khattach et al., 1995). This positive field test is based largely on the effect of unfolding on a single site (MX) with a positive in situ inclination, different from the low angle, negative inclinations that generally characterize the rest of the sites. Because the dispersion of the directions in these negative inclination sites (10 sites) does not greatly change with unfolding, we view this result with skepticism, principally because of the clear overlap with the P–T remagnetization direction.

The most certain period for West African paleogeography occurs at the end of the Neoproterozoic, constrained by virtue of the Adma intrusion pole (W4) and the slightly younger Tabankort rhyolite pole (W5) studied by Morel (1981). U–Pb dating of zircons extracted from diorite and adamellite of Adma instrusion yielded ages at 616 ± 11 and 613 ± 3 Ma, respectively. The next viable pole derives from the study of the Cambrian-Ordovician Hasi-Messaud sediments by Bucur (1971). The anchor provided by this pole (W14) for terminal Cambrian times coincides with the Cambro-Ordovician sector of the composite Gondwana APW path (McElhinny et al., 2003), the endpoint for the drift history in our analysis.

For the Amazon craton, only three paleomagnetic poles are available for the entire time interval considered in this work. A high-quality pole ($Q = 5$) is available for the flat-lying gabbros and associated basalts of the 1198 Ma Nova Floresta volcanics (A1) which records the position of the Amazon craton for the beginning of the Rodinian interval (Tohver et al., 2002). The other two poles derive from a recent paleomagnetic study of Neoproterozoic cap carbonates (Trindade et al., 2003). The dolomites and limestones of the Puga Fm. from the SE Amazon craton preserve two paleomagnetic components: a dual-polarity component that is observed at the base of the carbonate sequence, interpreted as a primary magnetization (pole A2); and a single-polarity, secondary (negative fold test) component obtained upsection along the more than 700 m thick succession of carbonates (pole A3). Although direct ages for the Puga sediments are not yet available, $^{87}Sr/^{86}Sr$ ratios and $\delta^{13}C$ results presented by Alvarenga et al. (2004) suggest to correlation with the ca. 630 Ma, post-glacial Marinoan units of the Congo craton (Hoffmann et al., 2004). The younger component gives a paleomagnetic pole (A3) that coincides with the remagnetized São Francisco carbonates mean pole (S17), and a new, high-quality pole for the Itabaiana dikes (B4) that dated at 525 Ma, as discussed below (Trindade et al., 2006).

As with the combined São Francisco–Congo craton, similarities in the geologic evolution of West Africa and the Amazon have long been used to infer a pre-Gondwanan link between the now separate cratons (Torquato and Cordani, 1981; Villeneuve and Cornée, 1994). The similar Paleoproterozoic and Mesoproterozoic paleomagnetic record from each unit reinforces this supposition (Onstott and Hargraves, 1981; Nomade et al., 2003). However, for the time window considered here, only the ca. 600 Ma Adma diorite (W4) and Tambankort rhyolite (W5) poles from West Africa and the component A of the Puga cap carbonates (A2, ca. 630 Ma) from the SW Amazon craton show ages that are comparable. In determining the general outline of the APW path of the greater Amazon–West African craton for this time, a conceded difficulty with the Puga A pole lies in the similarity of its paleomagnetic direction with the present-day field, suggesting to some workers (e.g. Macouin et al., 2004; Kilner et al., 2005) that it is the result of secondary remagnetization. Although preliminary stability tests on other sections of the Puga Fm. have confirmed the reversals found by Trindade et al. (2003), borne by detrital hematite (Font et al., 2005), the option to use or exclude the Puga A pole does not affect our eventual conclusions regarding the separate drift history of Amazonia–West Africa versus the other West Gondwanan blocks. This drift history is established principally by the ca. 600 Ma Adma diorite (W4) and Tabankort rhyolite (W5) poles, followed by the Puga B pole (A3) of Trindade et al. (2003). The mid-Cambrian age of this latter pole is established by proximity with reliable mid-Cambrian results (Itaibaiana dikes, B4; and Ntonya Ring, N12, discussed below). On a final note, subsequent deflection of the Puga B component along the curved Paraguay belt of the SE Amazon craton reported by Tohver et al. (2004c) suggests a mid-Cambrian upper limit for final suturing of the West Africa–Amazonia with the central Gondwanan Sao Francisco–Congo craton, a conclusion to be explored in more detail below.

### *2.4. Rio de la Plata and Luís Alves*

Most of the exposed portion of the Rio de la Plata Craton is found in Uruguay with a southern extension observed in the region of Buenos Aires, Argentina, and another exposed portion extending northward into the state of Rio Grande do Sul, southernmost Brazil (e.g. Dalla-Salda et al., 1988; Cingolani and Dalla Salda, 2000). Exposures of the Paleoproterozoic shield rocks of the Luís Alves Block found in the southern Brazilian states of Santa Catarina and Paraná are separated from the Rio de la Plata craton by the younger, Phanerozoic sedimentary and basaltic rocks of the Paraná Basin. The Luíz Alves craton is probably the northernmost extension of the Rio de la Plata Craton (Cordani et al., 2000), a hypothesis that awaits testing by geophysical observation of subsurface geology. For the time being, we accept this hypothesis implicitly by collating the paleomagnetic record of these two cratonic domains together. Very few paleomagnetic poles are presently available for the greater cratonic area (Fig. 2d), some of them with good geochronological ages but of low quality paleomagnetic and tectono-structural control (e.g. poles RP3, RP5, RP6, LA1). Only three poles can be considered sufficiently reliable ($Q \geq 5$) to be used in tracing an APWP for the Rio de la Plata-Luís Alves Craton (poles RP1, LA2, RP7). The pole RP1, obtained for sedimentary rocks from the La Tinta Formation, is the oldest reliable pole (Valencio et al., 1980). The presence of a normal and reversed polarity magnetic directions from the sampled stratigraphic column suggests a primary origin for the magnetization, dated at $709 \pm 24$ Ma by Rb–Sr analysis of diagenetic clay. The pole LA2 was obtained for the Campo Alegre Formation (D'Agrella-Filho and Pacca, 1988), with a U–Pb zircon age of 598 ± 29 Ma recently obtained for these volcanic rocks (Basei et al., 1998; Citroni et al., 2001). Finally, pole RP7 derives from a recent study of volcanic rocks from the Sierra de las Animas volcano-sedimentary sequence (Sánchez-Bettucci and Rapalini, 2002). Although geochronological constraints on the RP7 pole are poor, a tectonostratigraphic correlation based on associated glacial sediments and a paleopole position consistent with the Sinyai Dolerite (N8) and Mirbat Sandstone (N10) after restoration to Gondwanan coordinates (discussed below) suggest an age of ca. 550 Ma.

Fig. 6 suggests a possible APW track between 720 and 550 Ma joining the three poles cited above as recently proposed by Sánchez-Bettucci and Rapalini (2002). A preliminary virtual geomagnetic pole (VGP) obtained for the ∼600 Ma glacigenic Playa Hermosa Formation (RP2) by these authors agrees with the Campo Alegre (LA2) pole of similar age. The pole RP2 suggests that the glaciogenic deposits of Playa Hermosa could have been produced at low to intermediate latitudes. The younger portion of the APWP is poorly constrained by a magnetic overprint of the Sierra de las Animas magmatic complex (RP8). The age of this magnetization is tentatively interpreted as ca. 520 Ma, based on its similarity to other mid-Cambrian Gondwanan poles (Sánchez-Bettucci and Rapalini, 2002).

### *2.5. Arabian–Nubian shield and Brasiliano belts*

The average age of paleomagnetic directions reported from the Arabian/Nubian shield is considerably younger than results from the other tectonic units reviewed here (Fig. 2e), a fact that reflects the juvenile, Neoproterozoic genesis of this composite block. Paleomagnetic poles compiled from the Arabian–Nubian shield are widely scattered in terms of both position and age, which precludes a meaningful discussion of a unified APWP for a large portion of the time interval considered in this work. The same may be said for the record of the Brasiliano belts (Fig. 2f). The paleomagnetic record for times after 600 Ma gives some constraints on the post-accretionary history of the Arabian–Nubian terranes and illustrates the role of the stabilized shield in the final amalgamation of West Gondwana. We analyze both the Arabia–Nubian shield and Brasiliano mobile belt results together, in an attempt to stress the convergence of paths from both sides of central Gondwana by mid-Cambrian times.

For ages older than 600 Ma there is a high degree of geographic dispersion in Arabian–Nubian poles (Fig. 7), which reinforces the geological interpretation of multiple, far-traveled island arcs conjoined along Neoproterozoic suture zones (e.g. Stoesser and Camp, 1985; Stern, 1994; Abdel-Rahman, 1995; Windley et al., 1996). An alternative view presented by Meert and Torsvik (2003) suggests that the Arabian/Nubian shield is tectonically coherent with the São Francisco–Congo craton by ca. 840 Ma by virtue of the proximity (30° difference) of the Suakin gabbro pole (N1) of 841 ± 4 Ma ($^{40}Ar/^{39}Ar$ in hornblende) reported by Reischmann et al. (1992) and the 795 Ma Bukoban and Gagwe poles (C12, C16; see Fig. 4b) from Congo craton (Meert et al., 1995). Because the Suakin and Bukoban/Gagwe poles are of significantly different ages (ca. 50 Ma), it is impossible to say whether they record different time intervals of a single APW path for the greater São Francisco–Congo–Arabian craton or are unrelated records of two separate drift histories. Additionally, there is the possibility that the Suakin gabbro result might reflect a younger, 550 Ma remagnetization (see below). Given the sparseness of the paleomagnetic record, it seems reasonable to defer to abundant geological observations with regards to the significance of the multiple 900–600 Ma suture zones in the Arabian–Nubian shield (Stern, 1994). The timing of peak deformation and metamorphism along the greater Mozambique Belt occurred between 720 and 620 Ma, according to a recent geochronological review by Meert (2003), suggesting that poles younger than this may be considered as representative of a stable Arabian–Nubian craton. In view of these arguments, we suggest that the Arabian–Nubian shield was not a craton in the sense of having had a long history as a stable, coherent block prior to the events of the late Neoproterozoic (ca. 600 Ma).

For times after ca. 600 Ma, the oldest reliable pole for the Arabian–Nubian shield (Fig. 7) was obtained from studies of the Dokhan volcanics (N5) of Egypt (Davies et al., 1980; Nairn et al., 1987). This tilt-corrected result was derived from paleomagnetic study of rocks that have been recently dated at 593 ± 15 Ma by U–Pb analysis of zircon (Wilde and Youssef, 2000). Paleomagnetic results from the Nabati Complex (N7) reported by Saradeth et al. (1989) appear to confirm the approximate position of the Dokhan volcanics pole, in the southwestern portion of the modern Indian Ocean. This conclusion has been bolstered by a recent study of the glacial–interglacial sediments of late Neoproterozoic Huqf Gp. of Oman (N9) by Kilner et al. (2005). The primary nature of the remanence underpinning this high-quality result ($Q = 6$) is supported by the presence of reversals and a positive fold test, although the age of the sediments is imprecisely constrained to the 544–712 Ma interval. (The authors themselves suggest a Marinoan age, i.e. 580–600 Ma, for the glacial units in their study.) This new result supercedes an earlier paleomagnetic study (Kempf et al., 2000) of the glaciomarine Mirbat sandstones that occur in the upper portion of the Huqf Gp. Kempf et al. (2000) reported a paleomagnetic pole (N10) based on a low inclination direction found in ten samples from two sites. The declination of this direction is ~90° different from that reported by Kilner et al. (2005), perhaps reflective of a local rotation or an undetected hiatus in the sampled sequence. We note that the N9 pole is based on a direction isolated from a greater number of sample taken from three widely separate regions and appears to be more reliable. The fact that the N10 pole reported by Kempf et al. (2000) nearly coincides with the pole derived from study of the high-quality pole ($Q = 5$) from the Sinyai metadolerites (N8), precisely dated by $^{40}Ar/^{39}Ar$ analysis of biotite at 547 ± 4 Ma, suggests that the N10 result may be a ca. 550 Ma remagnetization. We note that the aforementioned Suakin gabbro (N1) pole also falls suspiciously close to these two 550 Ma poles, in spite of the significantly older age assigned to it. If the Suakin gabbro result is the product of remagnetization, this event must have occurred without disturbing the $^{40}Ar/^{39}Ar$ system in hornblende (plateau age of 841 ± 4 Ma) or biotite (plateau age of 782 ± 6 Ma), according to the age data reported by Reischmann et al. (1992). The record for the Brasiliano belts has no reliable entries for the 600–550 Ma interval.

A younger cluster of poles is found for ages between 530 and 510 Ma (Fig. 7). The age and position of this cluster is anchored by the Ntonya Ring pole of Malawi (N11) that constrains the position of the Arabian–Nubian block *senso latu* at 522 ± 13 Ma (Briden et al., 1993), an age established from $^{40}Ar/^{39}Ar$ dating of hornblende and biotite. Similar poles of the same age from rocks within the Brasiliano belts include the high-quality ($Q = 7$) Itabaiana pole (B4), for which an $^{40}Ar/^{39}Ar$ age of 525 ± 5 Ma was determined from paleomagnetic sample material (Trindade et al., 2006). The possible progression of the APW path through the poles obtained from the Juiz de Fora (B10) and Piquete (B11) metamorphic rocks is suggested in spite of the lack of tight age constraints for these latter poles. The 500 Ma mean of K–Ar ages from the Piquete metamorphic rocks will be compared with forthcoming $^{40}Ar/^{39}Ar$ ages for the Juiz de Fora rocks, the dating of which is currently in progress. A paleomagnetic pole (B7) obtained from syn-tectonic granites of the Seridó Belt to the NW of the São Francisco craton (Trindade, 1999) occupy an intermediate position between the Ntonya Ring and Itabaiana poles (N10, B4), and the Juiz de Fora pole (B10). Two K–Ar ages were obtained on biotite grains from these plutons at 527.3 ± 9.8 and 521.5 ± 14.6 Ma by Trindade (1999), interpreted as the age of magnetization acquisition. We note that the paleomagnetic pole for the similarly-aged Madagascar stratoid granites overlaps the Seridó granite pole after restoration of Madagascar to mainland African coordinates (Meert et al., 2003). All these poles with ages younger than 600 Ma define the best contrained APW segment (highlighted in Fig. 7) for West Gondwana at end Neoproterozoic/early Cambrian times.

## 3. Discussion

Our review of the West Gondwana paleomagnetic database covers a time interval that straddles the assembly and demise of the Rodinia supercontinent, followed closely by the amalgamation and the stabilization of the Gondwanan continent. Most prominent Rodinia reconstructions emphasize a suture between West Gondwanan cratonic elements and the eastern, Grenvillian margin of Laurentia (Hoffman, 1991; Dalziel, 1991). According to this hypothesis, the unified cratonic elements of Rodinia occupied a single, quiescent plate throughout the ca. 500 millions of years after the Grenville orogen and prior to the opening of the Iapetus ocean. Given the reference frame established by the Laurentian drift history compiled from Hyodo and Dunlop (1993), Meert et al. (1993), Weil et al. (1998) and Tohver et al. (2002), a comparison of the drift histories for each craton relative to Laurentia should reveal a common Rodinian paleogeography through similarities in latitude and orientation through time (Fig. 8). To this end, we use the reliable paleomagnetic data reviewed here to calculate the paleolatitude for a reference point within each craton, together with the orientation of the craton relative to present-day North at the time that the paleopole was recorded. The calculated position is compared to the drift history of Laurentia, calculated for two widely separated points on the Grenville margin of Laurentia, the Llano region of central Texas and Labrador, NE Canada (Fig. 8).

### 3.1. Rodinia

In examining the collective paleomagnetic record from all the major cratons of West Gondwana, we arrive at very different conclusions with respect to possible involvement in Rodinia. In some cases, the paleomagnetic data confirm latitudinal motions (Kalahari), whole scale rotations (São Francisco–Congo), or a lack of tectonic coherence (Arabia–Nubia) that are at odds with the established Laurentian drift history, evidence that these cratons were not located on the same plate as Laurentia

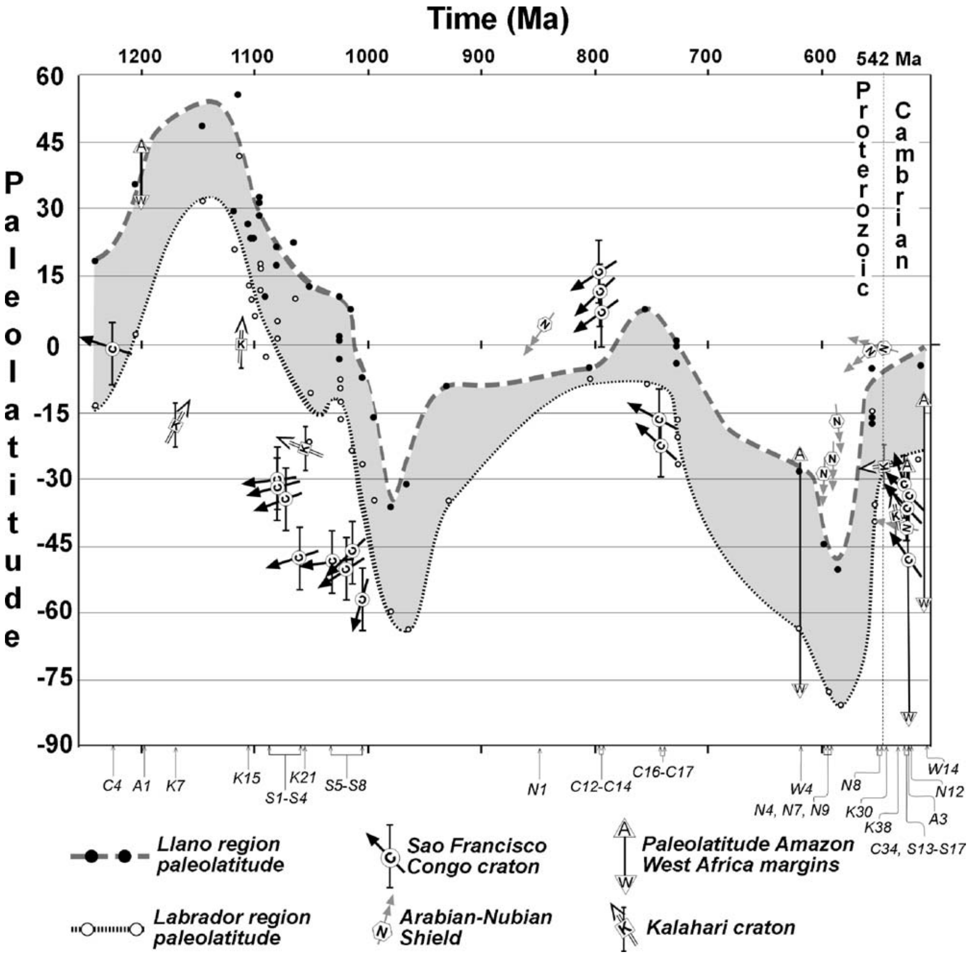


Fig. 8. Drift history for individual cratons of West Gondwana showing the latitude and orientation (declination) predicted for each based on reliable, well-dated paleomagnetic poles ($Q \geq 3$) used in the construction of segments of the APWPs shown in Figs. 3–7. Vertical error bars depict generic N-S extent of the individual cratons with arrows indicating the orientation, relative to the modern position. The shaded grey area is the position of the Grenville Province of Laurentia at its extreme ends: Labrador province, NE Canada—dotted black line; and Llano Uplift, Texas—grey, dashed line, according to paleomagnetic poles compiled from Hyodo and Dunlop, 1993; Meert et al., 1993; McCausland and Hodych, 1998; Weil et al., 1998; Tohver et al., 2002). Observe that the latitudinal swath covered by the Grenville province varies according to the orientation of Laurentia, which was rotated nearly 90° clockwise from the modern position throughout most of this period. There is a clear latitudinal separation between the São Francisco–Congo cratons and Laurentia for well-resolved time periods (e.g. 1100–1000 Ma, ca. 800 Ma), similar to the 1150–1050 Ma separation between Laurentia and the Kalahari. This separation and the generally divergent drift histories suggest that the São Francisco–Congo and Kalahari cratons were not located on a common plate as part of Rodinia. Note that Laurentia and West Africa-Amazon appear to part company with the opening of Iapetus between 600 and 500 Ma, although the precise timing is poorly resolved. The geographic coherence of West Gondwanan blocks, in terms of both latitude and orientation, is obvious only after the beginning of the Cambrian, suggesting that assembly of West Gondwana was not complete until after the beginning of Phanerozoic times.

(Fig. 8). In contrast, a Grenvillian suturing between the Amazon (plus West Africa) and Laurentia is supported by paleomagnetic data.

Extensive paleomagnetic study of the Kalahari craton is reflected in a well-defined APW path for the ca. 1165–1050 Ma interval, anchored by several high-quality paleomagnetic poles of a well-established age. This time interval coincides exactly with the robust paleomagnetic results established by study of the Keweenawan rocks of Laurentia (reviewed by Halls and Pesonen, 1982), the precise chronology of which has been established by detailed U–Pb work (e.g. Davis and Paces, 1990; Davis and Green, 1997). The high-quality data from both cratons allows for rigorous testing of the hypothesis that the Kalahari was the "missing southern continent" responsible for "Grenvillian" deformation of southern Laurentia (Dalziel et al., 2000). Two different analyses have been used to assess the alleged connection: the comparison of individual poles deemed to be reliable (e.g. Buchan et al., 2000; Hanson et al., 2004), and by matching APW paths of similar age and shape (Weil et al., 1998; Powell et al., 2001; Meert and Torsvik, 2003) where the drift history between reliable data points is extrapolated. Both analyses reveal a clear paleogeographic mismatch between the Kalahari and Laurentian cratons manifest in the 3000 ± 1400 km distance between the two continents (Dalziel et al., 2000; Powell et al., 2001), as well as the 90° misorientation of the "Grenvillian" mobile belts (Hanson et al., 2004). Observed discrepancies in the geological histories of the two belts (Tohver et al., 2005b) also suggest that the Kalahari was not contiguous with ancestral North America during the late Mesoproterozoic times. Our own analysis of the latitudinal drift (Fig. 8) demonstrates a geographic gap that ranges in magnitude from 1500 to 6000 km during the Grenvillian interval (1200–1000 Ma).

Our review of the São Francisco–Congo with respect to the single plate Rodinia hypothesis, although not conclusive, strongly suggests that this unit did not take part in Rodinia. Weil et al. (1998) suggested that the São Francisco–Congo and Laurentian cratons have similar APW paths marked by cusps at 1000–950 Ma, implying that both cratons could have occupied a single, common tectonic plate in Meso-Neoproterozoic times. However, as noted before, the exact time of the cusp and subsequent loop for the São Francisco–Congo path relies solely on the suspect Nyabikere VGP (C6). When comparing the latitudinal variation of Laurentia and the São Francisco–Congo craton, our analysis shows that these units were not located at the same latitude throughout the Neoproterozoic, with the SFC 1500–3000 km further south during the 1100–1000 Ma, and ca. 1000 km north of the Grenville margin of Laurentia at ca. 800 Ma. (Fig. 8). The possibility of a distal link between Laurentia and the São Francisco–Congo craton (e.g. with Amazonia–West Africa sandwiched between) is dispelled by observations of the ca. 90° rotation that affected the São Francisco–Congo craton at 800–740 Ma, an event with no counterpart in the Laurentian drift history. Geological evidence reinforces the interpretation of separate evolutions for the São Francisco–Congo craton and Laurentia during Rodinian times (e.g. Kröner and Cordani, 2003; Cordani et al., 2003). Notably, the Grenville-aged Carirís Velhos belt located north of the São Francisco craton records dominantly extensional processes (Brito Neves et al., 2000; Neves, 2003), in clear contrast with the collisional history of the Laurentian Grenville orogen.

Of all the units considered here, the Amazon craton is the only one considered to have any direct connection to Laurentia. The hypothesized collision between Laurentia and Amazonia was originally advanced on the basis of matching the Sunsas belt of eastern Bolivia with the central Grenville belt, i.e. Ontario-New York (e.g. Sadowski and Bettencourt, 1996). Paleomagnetic data from Amazonia presented by Tohver et al. (2002) demonstrate the similarity between the orientation of "Grenvillian" mobile belts and paleolatitudinal positions of Amazonia and southern Laurentia at the beginning of the Grenville interval (1200 Ma). The geometry of this Llano–Amazon collision at ca. 1.2 Ga is supported by a comparison of the resultant metamorphic history on both sides of the orogenic zone (Tohver et al., 2005b). After the original collision, an evolving configuration of the relative position of Amazonia along-strike of the Grenville margin of Laurentia has been suggested on the basis the two separate stages of tectonometamorphism observed within the SW Amazon craton, the sinistral, strike-slip offsets associated with each tectonic pulse (Tohver et al., 2004a, 2005a), as well as isotopic evidence for an Amazonian terrane within the SE Appalachians, ca. 1000 km ENE of the original collisional zone (Loewy et al., 2003; Tohver et al., 2004b). Unfortunately, the present lack of paleomagnetic data for the Amazon–West Africa craton from the Grenvillian interval after 1.2 Ga prevents us from discerning the details of this hypothesized change in the West African–Amazon–Laurentia geometry.

The paleomagnetically determined position of West Africa–Amazonia relative to Laurentia does favor a common Rodinian paleogeography for times after 1200 Ma through ca. 600 Ma (Fig. 9), the age of the Adma diorite (W4). For latest Neoproterozoic times, Laurentia's drift from high, southerly latitudes towards the equator by mid-Cambrian times appears incontrovertible, regardless of the debate surrounding the timing of this motion (c.f., Meert et al., 1993; Kirschvink et al., 1997; McCausland and Hodych, 1998; Pisarevsky et al., 2001; Meert et al., 2001; Hodych et al., 2004). In contrast, the Amazon–West Africa craton appear to be relatively stationary between 600 Ma until the end of Cambrian times, as seen from the short length of the 600–525 Ma APW path. Therefore, the Amazon–West Africa craton does not accompany the rapid drift history of Laurentia towards the equator at this time. This can be seen in Fig. 8 as Amazonia strays away its previous position along the (then) northernmost extent of the Laurentian Grenville margin (cf. pole A2), reflecting the opening of the Iapetus ocean between Amazonia and Laurentia. The exact timing of this opening is imprecisely resolved by the paleomagnetic data from the Amazon–West African craton, which are available only for latest Cambrian times (Fig. 10).

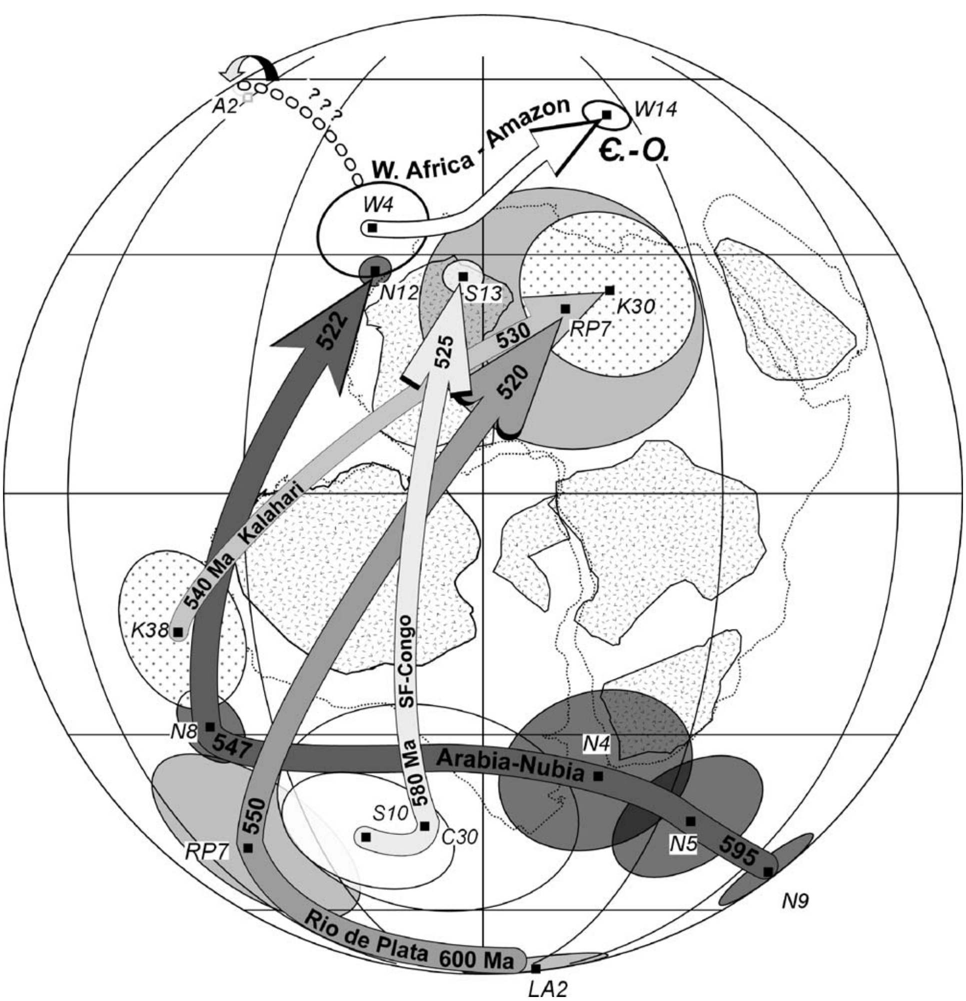


Fig. 9. Junction of apparent polar wander paths for each of the cratonic elements of central Gondwana vs. the separate drift history of Amazonia-West Africa until mid Cambrian times as discussed in text.

### *3.2. Rodinia to Gondwana*

The transition from Rodinia to Gondwana is recorded by the convergence of all individual APW paths for West Gonwana cratons by mid-Cambrian times. Two separate trends in the paleomagnetic data are clear for the cratonic units of greater West Gondwana: the early assembly (550–580 Ma) of the cratons of central Gondwana: São Francisco–Congo, Kalahari, Rio de la Plata, and Arabia–Nubia; and the late (mid-Cambrian) collision of these blocks with West Africa–Amazonia. Regarding this first point, the proximity of poles from the São Francisco–Congo, Kalahari, Rio de la Plata, and Arabia–Nubia shield near Patagonia/South Africa (in African coordinates) suggest a common APW path by ca. 550 Ma (Fig. 9), suggesting that the central blocks of West Gondwana were assembled by that time. Before 550 Ma, the differences in pole positions between the various central Gondwanan cratons may reflect divergent APW paths or different-aged portions of a common APW path. For example, the APW path for the São Francisco–Congo craton may be traced back to 580 Ma based on the poles S10 and C30 (Fig. 4b) which are close to, but do not overlap the Dokhan volcanics pole from the Arabian–Nubian dataset of slightly older age, ca. 595 Ma (N4, N5). Another example is the ca. 25° distance observed between these poles and the ca. 590 Campo Alegre pole (L2 in Fig. 6) of the Rio de la Plata–Luis Alves dataset, a difference that might reflect separate paleogeographic locations or poor age assignments to poles on the same APW path. The separate evolution of these blocks until at least 550 Ma would contradict the classical view of West Gondwana assembly being complete by ca. 600 Ma (e.g. Trompette, 2000).

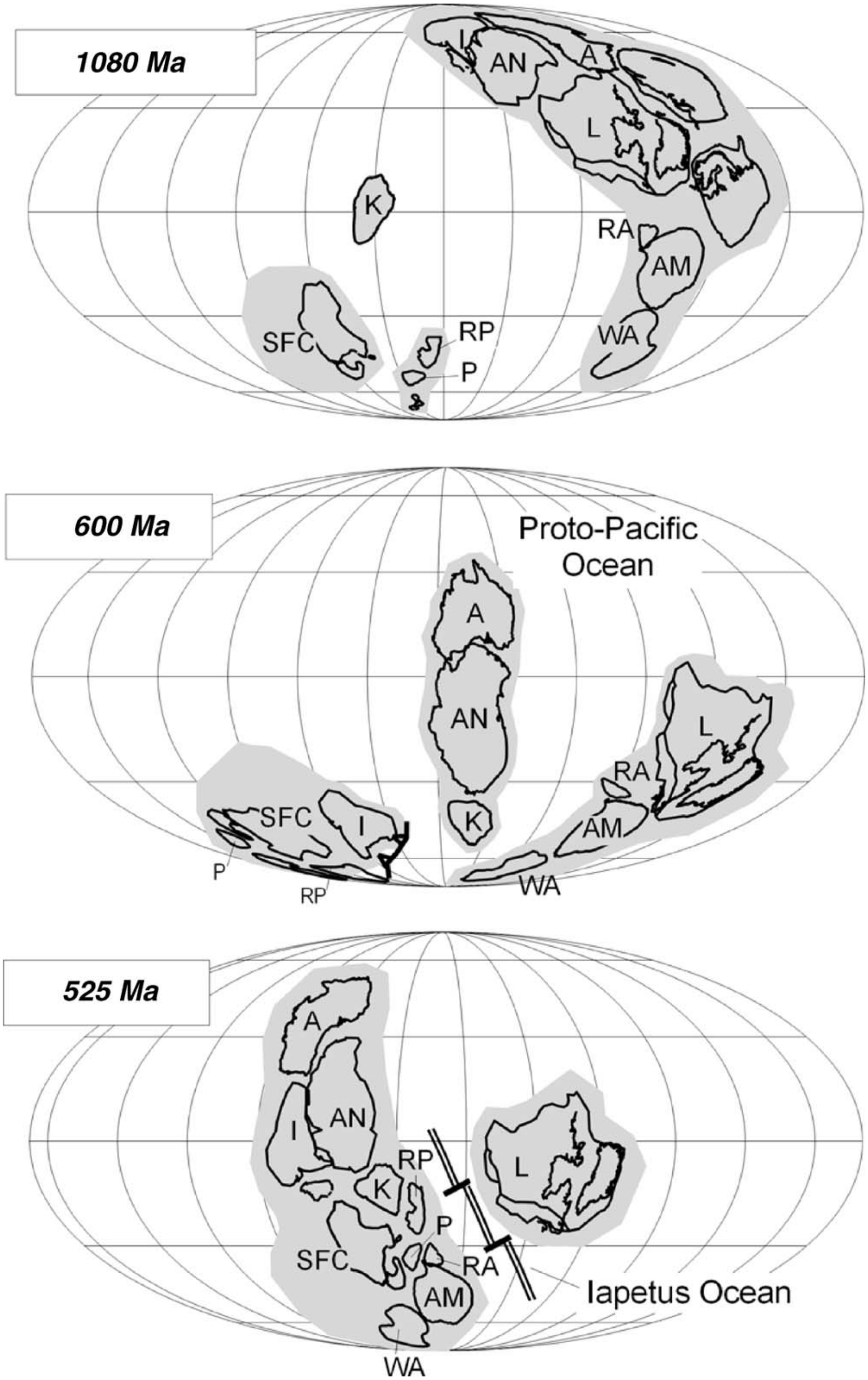


Fig. 10. Paleogeographic reconstructions based on the paleomagnetic data reviewed in this contribution: the Rodinia supercontinent at 1080 Ma, followed by break-up along the western margin of Laurentia by 600 Ma (opening of the proto-Pacific Ocean), and final splintering along the eastern margin of Laurentia (opening of the Iapetus ocean) by 525 Ma. Laurentian poles used in the 1080 Ma reconstruction are listed in D'Agrella-Filho et al. (2004b). The position of Laurentia at 600 and 525 Ma is based on the Long Range dykes pole and the Tapeats sandstone pole, respectively.

Geochronological data from the exhumed, high grade mobile belt that marks the S. American/African suture (Mantiqueira/Ribeira and Dom Feliciano belts, Fig. 1) is increasingly abundant and reveals an intriguing trend towards younger ages in the central part of the Ribeira belt, 620–520 Ma (e.g. Machado et al., 1996; Schmitt et al., 2004) versus the southern Dom Feliciano belt, located on the eastern margin of the Rio de Plata/Luis Alves craton, where crystallization ages range from 750 to 600 Ma (e.g. Babinski et al., 1996; Basei et al., 2000). The geological implication that the Kalahari/Rio de Plata collision occurred before joining the São Francisco–Congo craton is permissible, using the paleomagnetic data presently available (Fig. 9). A recent review of the geochronological record from southern Africa corroborates this view of a separation between the Kalahari and Congo cum São Francisco craton until Cambrian times (Johnson et al., 2005).

The second major observation regards the separate drift record for the Amazon–West African craton from that observed for the central Gondwanan cratons. Regardless of whether one accepts the Puga A2 pole as primary, the short length and position of the APW path defined between poles the Adma diorite W4, Tabankort rhyolite (W5) and the remagnetized Puga result (A3) contrasts strongly with long, 60–90° segments recorded by the central Gondwanan blocks. The Iapetan rifting that resulted in rapid drift on the part of Laurentia was marked by much less dramatic motion on the part of the Amazon–West African craton. Coherence of the Amazon–West Africa paleomagnetic dataset with the APW paths of the central Gondwanan cratons becomes clear by ca. mid-Cambrian times. Given these observation, we interpret the Amazon craton and minor adjoining blocks, such as the Rio Apa and Pampia, to have collided with the central Gondwana by ca. 530–520 Ma. This scenario is supported by geological evidence pointing to a protracted collision at the (present-day) western border of the São Francisco craton and eastern margin of Amazonia, suggested by Campanha and Brito Neves (2004) to be the result of a series of orthogonal collisions. Neoproterozoic juvenile arcs with crystallization ages varying from 940 to 600 Ma were recognized between the São Francisco craton and the Central Goias block (Pimentel and Fuck, 1992; Pimentel et al., 2000; Laux et al., 2005), signifying that a considerable, ancient ocean basin divided the present-day western border of São Francisco–Congo craton from the Amazon–West African cratonic blocks. Younger isotopic ages in the 580–500 Ma range record deformation associated with the closing of this basin along the Brasilia belt (Pimentel et al., 1996; Valeriano et al., 2004), Araguaia belt (Herz et al., 1989), and Paraguai belt (Alvarenga et al., 2000) at a time when Amazonia–West Africa were presumably rifting away from Laurentia. Paleomagnetic evidence for rotations accompanying the formation of the curvilinear Paraguay belt places a mid-Cambrian upper limit on the timing of deformation (Tohver et al., 2004c). Limited rifting within the São Francisco–Congo junction led to the development of a relatively restricted oceanic domain recorded by ophiolitic remnants dated at 800 Ma (Pedrosa-Soares et al., 1998, 2001; Tack et al., 2001). Most of these regions were progressively deformed and metamorphosed during the successive Panafrican/Brasiliano collisions, thus erasing the magnetic record of these events.

## 4. Conclusions

Our review of the paleomagnetic database for western Gondwana for 1200–500 Ma reveals major hiatuses in the record of the drift history for all the major cratons. The limited intervals of time where the APW path can be reliably determined prevent overly rigorous assessments of the paleogeography of Rodinia. However, clear differences in the drift histories that can be reliably established from the established motion of Laurentia during Meso-Neoproterozoic times suggest that most of these blocks (i.e. Kalahari, São Francisco–Congo, Arabian–Nubian shield) were not part of Rodinia. These cratons of central Gondwana appear to have converged and collided sometime around 550–580 Ma, as indicated by a common APW after that time. In contrast, the available paleomagnetic data for the Amazon–West African craton suggests a parallel motion with Laurentia, demonstrating that these cratons were sutured across a greater Grenville mobile belt. The transition from Rodinia to a united west Gondwana appears to have taken place between 600 Ma, when Amazonia–West Africa was still sutured to Laurentia, and ca. 520 Ma, when convergence with paleomagnetic poles from the other cratons is observed. Based on this, we suggest a two stage collisional process for the construction of West Gondwana, an early phase marked by the assembly of the central Gondwana cratons (Kalahari, São Francisco–Congo, Arabian–Nubian shield) followed by a mid-Cambrian collision with the westernmost craton Amazonia–West Africa.

## Q&A section

Question: Taking the paleomagnetic constraints you have documented for ∼630 Ma to Cambrian time, what was the geometry of the Amazonia-West Africa closure and collision with Congo-Sao Francisco/Kalahari/Rio de la Plata during the assembly of West Gondwana? On the 'global' scale, was it dominantly orthogonal or strike-slip?

Tohver answers:

Reconstructing the kinematic history between two independent plates (and the consequent "angle of approach" between continents on these plates) using only paleomagnetic data is difficult because of the longitudinal uncertainty inherent to paleomagnetic data. The problem lies in the difference between paleomagnetic pole, which is a proxy for the geographic spin axis of the Earth, and the Euler pole, which describes the plate motion of an individual plate on the Earth's surface. An increased distance between the paleomagnetic pole and the Euler pole will result in greater fidelity between the length of the APWP and actual continental motion, resolved through paleolatitude (though not paleolongitude, which remains unknown). The opposite obtains in cases where the geographic and Euler poles coincide, in which case a continent may be spinning about the geographic/Euler pole with no motion apparent from the resultant APWP, which would be of zero length.

In the specific case of tracking the convergence of the Amazon-West African plate with the already-fused plate comprising the central Gondwana blocks (Congo-São Francisco and Kalahari), the convergence of the APWPs appears to have occurred by mid-Cambrian times. The comparatively short length of the Amazon-West African APWP from 600 to 520 Ma suggests slow latitudinal drift rates, compared with the long track length of the central Gondwanan blocks from the same time period, suggestive of higher drift rates. This information, taken by itself, does not reveal anything about the relative motions that characterized the collision zone. Such information is better reconstructed using the more traditional methods for finding Euler poles: reconstructing small circles about the Euler pole by identifying transform (or strike-slip) boundaries, or calculating great circles on the basis of segments of collisional belts dominated by orthogonal convergence. A preliminary exercise carried out by Campanha and Brito Neves (2004) suggests that the collision between western (Amazon-West Africa) and central portions (Congo-São Francisco and Kalahari cratons) of Gondwana was dominated by orthogonal convergence, with isolated segments marked by strike-slip motions. One problem that this latter approach may present is the unrecognized effect of local rotations on strain fabrics, and a resultant tendency to confuse the orientation of the finite strain ellipsoid with the orientation of the principal stress directions.

## Acknowledgments

E. Tohver received support from the National Science Foundation (#INT-0301807) while preparing this contribution. M. D'Agrella-Filho and R. Trindade received support from the Fundação de Amparo à Pesquisa do Estado de São Paulo (#98/3621-4 and 03/12802-2). Thoughtful reviews by Valerian Bachtadse and Ken Buchan and the many suggestions by Richard Hanson regarding the geology of the Kalahari craton improved the original manuscript. The painstaking editorial work of Phil McCausland prevented numerous errors from being incorporated into the final text and is greatly appreciated.

## References

Abdel-Rahman, A.M., 1995. Tectonomagmatic stages of shield evolution: the Pan-African shield in northeastern Egypt. Tectonophysics 242, 223–240.

Abdeldayem, A.L., Kafafy, A.M., Tarling, D.H., 1994. Paleomagnetic studies of some sediments, southwest Sinai, Egypt. Tectonophysics 234, 217–225.

Allsop, H.L., Bristow, J.W., Smith, C.B., Brown, R., Gleadow, A.J.W., Kramers, J.D., Garvie, O.G., 1989. A summary of radiometric dating methods applicable to kimberlites and related rocks, 343–357. In: Ross, J. (Ed.), Kimberlites and Related Rocks, Vol. I: Their Composition, Occurrence, Origin and Emplacement. Proceedings of the Fourth International Kimberlite Conference, Perth, 1986. Geol. Soc. Austr. Spec. Publ. 14, 1–646.

Alvarenga, C.J.S., Veloso Moura, C.A., Sousa Gorayeb, P.S., Matos de Abreu, F.A., 2000. Paraguay and Araguaia belts. In: Cordani, U.G., Milani, E.J., Thomaz Filho, A., Campos, D.A. (Eds.), Tectonic Evolution of South America, 31st International Geological congress. Rio de Janeiro, Brazil, pp. 183–193.

Alvarenga, C.J.S., Santos, R.V., Dantas, E.L., 2004. C–O–Sr isotopic stratigraphy of cap carbonates overlying Marinoan-age glacial diamictites in the Paraguay Belt, Brazil. Precam. Res. 131, 1–21.

Babinski, M., Chemale, F., Hartmann, L.A., van Schmus, W.R., da Silva, L.C., 1996. Juvenile accretion at 750–700 Ma in southern Brazil. Geology 24, 439–442.

Basei, M.A.S., Citroni, S.B., Siga Jr., O., 1998. Stratigraphy and age of fini-proterozoic basins of paraná and santa catarina states, Southern Brazil. Bol. Inst. Geoc. 29, 195–216.

Basei Jr., M.A.S., Siga, O., Masquelin H., Harara, O.M., Reis Neto, J.M., Preciozzi, F.P., et al., 2000. The Dom Feliciano belt of Brazil and Uruaguay and its foreland domain, the Rio de Plata craton. In: Cordani, U.G., Milani, E.J., Thomaz Filho, A., Campos, D.A. (Eds.), Tectonic Evolution of South America, 31st International Geological Congress. Rio de Janeiro, Brazil, pp. 311–344.

Briden, J.C., 1968. Paleomagnetism of the Ntonya Ring Structure. Malawi. J. Geophys. Res. 73, 725–733.

Briden, J.C., Duff, B.A., Kröner, A., 1979. Palaeomagnetism of the Koras Group, Northern Cape Province, South Africa. Precam. Res. 10, 43–57.

Briden, J.C., McClelland, E.A., Rex, D.C., 1993. Proving the age of a palaeomagnetic pole: the case of the Ntonya ring structure, Malawi. J. Geophys. Res. 98, 1743–1749.

Brito Neves, B.B., Santos, E.J., Van Schmus, W.R., 2000. Tectonic history of the Borborema province, northeastern Brazil. In: Cordani, U.G., Milani, E.J., Thomaz Filho, A., Campos, D.A. (Eds.), Tectonic Evolution of South America, 31st International Geological congress. Rio de Janeiro, pp. 151–182.

Brock, A., 1967. Palaeomagnetic result from the Hook Intrusives of Zambia. Nature 216, 359–360.

Brock, A., Raja, P.K.S., Vise, J.B., 1972. The palaeomagnetism of the Kisii Series, western Kenya. Geophys. J. Roy. Astron. Soc. 28, 129–137.

Buchan, K.L., Mortensen, J.K., Card, K.D., 1994. Integrated paleomagnetic and U–Pb geochronologic studies of mafic instrusions in the southern Canadian Shield. Precam. Res. 69, 1–10.

Buchan, K.L., Mertanen, S., Park, R.G., Pesonen, L.J., Elming, S.Å., Abrahamsen, N., Bylund, G., 2000. Comparing the drift of Laurentia and Baltica in the Proterozoic: the importance of key palaeomagnetic poles. Tectonophysics 319, 167–198.

Buchan, K.L., Ernst, R.E., Hamilton, M.A., Mertanen, S., Pesonen, L.J., Elming, S.Å., 2001. Rodinia: the evidence from integrated paleomagnetism and U-Pb geochronology. Precam. Res. 110, 9–32.

Bucur, I., 1971. Etude paleomagnetique d'une formation sedimentaire du Sahara algerien, d'age Cambro-Ordovicien. Ann. Geophys. 27, 255–261.

Campanha, G.A.C., Brito Neves, B.B., 2004. Frontal and oblique tectonics in the Brazilian shield. Episodes 27, 255–259.

Carvalho, H., Tassinari, C.C.G., Alves, P.H., Guimarães, F., Simões, M.C., 2000. Geochronological review of the Precambrian in western Angola: links with Brazil. J. Afr. Earth Sci. 31, 383–402.

Cingolani, C., Dalla Salda, L., 2000. Buenos aires cratonic region. In: Cordani, U.G., Milani, E.J., Thomaz Filho, A., Campos, D.A. (Eds.), Tectonic Evolution of South America, 31st International Geological Congress. Rio de Janeiro, Brazil, pp. 139–147.

Citroni, S.B., Basei, M.A.S., Siga Junior, O., Reis Neto, J.M., 2001. Volcanism and stratugraphy of the Neoproterozoic Campo Alegre Basin, SC. An. Acad. Bras. Ciênc. 73, 581–597.

Cordani, U.G., Sato, K., Teixeira, W., Tassinari, C.C.G., Basei, M.A.S., 2000. Crustal evolution of the South American platform. In: Cordani, U.G., Milani, E.J., Thomaz Filho, A., Campos, D.A. (Eds.), Tectonic Evolution of South America, 31st International Geological Congress. Rio de Janeiro, Brazil, pp. 19–40.

Cordani, U.G., D'Agrella-Filho, M.S., Brito-Neves, B.B., Trindade, R.I.F., 2003. Tearing up Rodinia: the neoproterozoic palaeogeography of South American cratonic fragments. Terra Nova 15, 350–359.

Correia, P.B., Ernesto, E., 1998. Paleomagnetismo e idades K–Ar do Complexo Intrusivo Itaqui, Estado de São Paulo. Rev. Bras. Geochem. 28, 495–502.

Costanzo-Alvarez, V., Dunlop, D.J., 1998. A regional paleomagnetic study of lithotectonic domains in the Central Gneiss Belt, Grenville Province, Ontario. Earth Planet. Sci. Lett. 157, 89–103.

D'Agrella-Filho, M.S., 1992. Paleomagnetismo de enxames de diques máficos proterozóicos e rochas do embasamento do craton do São Francisco. PhD Thesis. Instituto de Astronomia e Geofisica, Universidade de Sao Paulo, Sao Paulo, Brazil, 201 pp.

D'Agrella-Filho, M.S., Pacca, I.G., 1988. Paleomagnetism of the Itajaí Castro and Bom Jardim Groups from Southern Brazil. Geophys. J. 93, 365–376.

D'Agrella-Filho, M.S., Pacca, I.G., Sato, K., 1986. Paleomagnetism of metamorphic rocks from the Piquete region—Ribeira Valley, Southeastern Brazil. Rev. Bras. Geofís. 4, 79–84.

D'Agrella-Filho, M.S., Pacca, I.G., Renne, P.R., Onstott, T.C., Teixeira, W., 1990. Paleomagnetism of middle proterozoic (1.01–1.18 Ga) mafic dikes in southeastern Bahia State—São Francisco Craton, Brazil. Earth Planet. Sci. Lett. 101, 332–348.

D'Agrella-Filho, M.S., Feybesse, J.-L., Prian, J.-P., Dupuis, D., N'Dong, J.E., 1996. Palaeomagnetism of Precambrian rocks from Gabon, Congo Craton, África. J. Afr. Earth Sci. 22, 65–80.

D'Agrella-Filho, M.S., Trindade, R.I.F., Siqueira, R., Ponte-Neto, C.F., Pacca, I.G., 1998. Paleomagnetic constraints on the Rodinia supercontinent: implications for its Neoproterozoic break-up and the formation of Gondwana. Int. Geol. Rev. 40, 171–188.

D'Agrella-Filho, M.S., Babinski, M., Trindade, R.I.F., Van Schmus, W.R., Ernesto, M., 2000. Simultaneous remagnetization and U–Pb isotope resetting in Neoproterozoic carbonates of the São Francisco craton, Brazil. Precam. Res. 99, 179–196.

D'Agrella-Filho, M.S., Raposo, M.I.B., Egydio-Silva, M., 2004a. Paleomagnetic study of the Juiz de Fora Complex, SE Brazil: implications for Gondwana. Gondwana Res. 7, 103–113.

D'Agrella-Filho, M.S., Pacca, I.I.G., Trindade, I.F., Teixeira, W., Raposo, M.I.B., Onstott, T.C., 2004b. Paleomagnetism and $^{40}Ar$–$^{39}Ar$ ages of mafic dikes from Salvador (Brazil): new constraints on the São Francisco craton APW path between 1080 and 1010 Ma. Precam. Res. 132, 55–77.

Dalla-Salda, L.H., Bossi, J., Cingolani, C.A., 1988. The Rio de la Plata cratonic region of Southwestern Gondwanaland. Episodes 11, 263–269.

Daly, L., Pozzi, J.P., 1977. Determination d'un nouveau pole paleomagnetique africain sur des formations cambriennes du Maroc. Earth Planet. Sci. Lett. 34, 264–272.

Dalziel, I.W.D., 1991. Pacific margins of Laurentia and east Antarctica–Australia as a conjugate rift pair: evidence and implications. Geology 19, 598–601.

Dalziel, I.W.D., Mosher, S., Gahagan, L.M., 2000. Laurentia–Kalahari collision and the assembly of Rodinia. J. Geol. 108, 499–513.

Davies, J., Nairn, A.E.M., Ressetar, R., 1980. The paleomagnetism of certain late Precambrian and early Paleozoic rocks from the Red Sea Hills, Eastern Desert. Egypt J. Geophys. Res. 85, 3699–3710.

Davis, D.W., Paces, J.B., 1990. Time resolution of geologic events on the Keweenawan Peninsula and implications for development of the Micontinent Rift system. Earth Planet. Sci. 97, 54–64.

Davis, D.W., Green, J.C., 1997. Geochronology of the North American midcontinent rift in western Lake Superior and implications for its geodynamic evolution. Can. J. Earth Sci. 34, 476–488.

Deblond, A., Punzalan, L.E., Boven, A., Tack, L., 2001. The Malagarazi supergroup of southeast Burundi and its correlative Bukoba supergroup of northwest Tanzania: Neo- and Meso-proterozoic constraints from Ar–Ar ages of mafic intrusive rocks. J. Afr. Earth Sci. 32, 435–449.

Doppelhammer, S.K., Hargraves, R.B., 1994. Paleomagnetism of the schuller and franspoort kimberlite pipes in south africa and an improved premier pole. Precam. Res. 69, 193–197.

Evans, D.A.D., Gutzmer, J., Beukes, N.J., Kirschvink, J.L., 2001. Paleomagnetic constraints on ages of mineralization in the Kalahari manganese field, South Africa. Econ. Geol. 96, 621–631.

Evans, D.A.D., 1998. True polar wander, a supercontinental legacy. Earth Planet. Sci. Lett. 157, 1–8.

Evans, D.A.D., 2000. Stratigraphic, geochronological, and paleomagnetic constraints upon the Neoproterozoic climatic paradox. Am. J. Sci. 300, 347–433.

Fairhead, J.D., 1988. Mesozoic plate tectonic reconstructions of the central South Atlantic ocean: the role of the west and central African rift system. Tectonophysics 155, 181–192.

Font, E., Trindade, R.I.F., Nédélec, A., 2005. Detrital remanent magnetization in haematite-bearing Neoproterozoic Puga cap dolostone, Amazon craton: a rock magnetic and SEM study. Geophys. J. Int. 163, 491–500.

Goldreich, P., Toomre, A., 1969. Some remarks on polar wandering. J. Geophys. Res. 74, 2555–2569.

Gose, W.A., Johnston, S.T., Thomas, R.J., 2004. Age of magnetization of Mesoproterozoic rocks from the Natal sector of the Namaqua–Natal belt, South Africa. J. Afr. Earth Sci. 40, 137–145, doi:10.1016/j.jafrearsci.2004.11.003.

Grotzinger, J.P., Bowring, S.A., Saylor, B.Z., Kaufman, A.J., 1995. Biostratigraphic and geochronologic constraints on early animal evolution. Science 270, 598–604.

Guerreiro, S.D.C., Sial, A.N., 1982. paleomagnetismo de um enxame de diques do Cambriano, na região de Sobral, Ceará. In: Anais do XXXII Congresso Brasileiro de Geologia, vol. 4, Salvador, Bahia, pp. 1609–1614.

Gutzmer, J., Beukes, N.J., Pickard, A., Barley, M.E., 2000. 1170 Ma SHRIMP age for koras group bimodal volcanism, northern cape province. South Afr. J. Geol. 103, 32–37.

Hailwood, E.A., 1972. Paleomagnetic studies on rock formation in the High Atlas and Ant-Atlas regions of Morocco. PhD Thesis. University of Newcastle, Tyne.

Hailwood, E.A., Tarling, D.H., 1973. Paleomagnetic evidence for a proto-Atlantic ocean. In: Tarling, D.H., Runcorn, S.K. (Eds.), Implications of Continental Drift to the Earth Sciences, vol. 1. Academic Press, London, pp. 36–37.

Halls, H.C., Pesonen, L.J., 1982. Paleomagnetism of Keweenawan rocks. Geol. Soc. Am. Mem. 156, 173–201.

Hanson, R.E., 2003. Proterozoic geochronology and tectonic evolution of southern Africa, In: Yoshida, M., Windley, B.F., Dasgupta, S. (Eds.), Proterozoic East Gondwana: Supercontinent Assembly and Breakup, Geol. Soc. Sp. Pub. 206, 427–463.

Hanson, R.E., Martin, M.W., Bowring, S.A., Munyanyiwa, H., 1998. U–Pb zircon age for the Umkondo dolerites, eastern Zimbabwe: 1.1 Ga large igneous province in southern Africa–East Antarctica and possible Rodinia correlations. Geology 26, 1143–1146.

Hanson, R.E., Vrowley, J.L., Bowring, S.A., Ramezani, J., Gose, W.A., Dalziel, I.W.D., Pancake, J.A., Seidel, E.K., Blenkinsop, T.G., Mukwakwami, J., 2004. Coeval large-scale magmatism in the Kalahari and Laurentia cratons during Rodinia assembly. Science 304, 1126–1129.

Hanson, R.E., Wardlaw, M.S., Wilson, T.J., Mwale, G., 1993. U–Pb zircon ages from the Hook granite massif and Mwembeshi dislocation: constraints on Pan-African deformation, plutonism, and transcurrent shearing in central Zambia. Precam. Res. 63, 189–209.

Hargraves, R.B., Hattingh, P.J., Onstott, T.C., 1994. Paleomagnetic results from the Timbavati Gabbros in the Kruger National Park, South Africa. S. Afr. J. Geol. 97, 1–5.

Herz, N., Hasui, Y., Costa, J.B.S., Matta, M.A. Silva, 1989. The Araguaia fold belt Brazil: a reactivated Brasiliano-Pan-African cycle (550 Ma) geosuture. Precam. Res. 42, 371–386.

Hoal, B.G., Heaman, L.M., 1995. The sinclair sequence: U–Pb age constraints from the Awasib mountain area. Geol. Surv. Namibia Commun. 10, 83–91.

Hodych, J.P., Cox, R.A., Kosler, J., 2004. An equatorial Laurentia at 550 Ma confirmed by Grenvillian inherited zircons dated by LAM ICP-MS in the Skinner Cove volcanics of western Newfoundland: implications for inertial interchange true polar wander. Precam. Res. 129, 93–113.

Hoffman, P.F., 1991. Did the breakout of Laurentia turn Gondwanaland inside-out? Science 252, 1409–1412.

Hoffman, P.F., Hawkins, D.P., Isachsen, C.E., Bowring, S.A., 1996. Precise U–Pb zircon ages for early Damaran magmatism in the Summas mountains and Welwitschia inlier, northern Damara belt, Namibia. Geol. Surv. Namibia Commun. 11, 47–52.

Hoffman, P.F., Kaufman, A.J., Halverson, G.P., Schrag, D.P., 1998. A Neoproterozoic snowball Earth. Science 281, 1342–1346.

Hoffmann, K.H., Condon, D.J., Bowring, S.A., Crowley, J.L., 2004. U–Pb zircon date from the Neoproterozoic Ghaub Formation, Namibia: constraints on Marinoan glaciation. Geology 32, 817–820, doi:10.1130/G20519.1.

Hyodo, H., Dunlop, D.J., 1993. Effect of anisotropy on the paleomagnetic contact test for a Grenville dike. J. Geophys. Res. 98, 7997–8017.

Ito, H., Tokeida, K., Suwa, K., Kume, S., 1978. Remanent magnetization of Precambrian and Cretaceous kimberlites in South Africa. Geophys. J. Roy. Astron. Soc. 55, 123–130.

Jacobs, J., Falter, M., Thomas, R.J., Kunz, J., Jessberger, E.K., 1997. $^{40}Ar/^{39}Ar$ thermochronological constraints on the structural evolutionof the Mesoproterozoic Natal Metamorphic Province, SE Africa. Precam. Res. 86, 71–92.

Johnson, S.P., Rivers, T., de Waele, B., 2005. A review of the Mesoproterozoic to early Palaeozoic magmatic and tectonothermal history of south–central Africa: implications for Rodinia and Gondwana. J. Geol. Soc. 162, 433–450.

Jones, D.L., 1968. Paleomagnetism of the premier mine kimberlite. J. Geophys. Res. 73, 6937–6944.

Jones, D.L., McElhinny, M.W., 1966. Paleomagnetic correlation of basic intrusions in the Precambrian of southern Africa. J. Geophys. Res. 71, 543–552.

Jones, D.L., McFadden, P.L., Kröner, A., McWilliams, M.O., 1992. Palaeomagnetic results from the late Precambrian Chela Group of southwest Angola. Precam. Res. 59, 1–13.

Kempf, O., Kellerhals, P., Lowrie, W., Matter, A., 2000. Paleomagnetic directions in Late Precambrian glaciomarine sediments of the Mirbat Sandstone Formation, Oman. Earth Planet. Sci. Lett. 175, 181–190.

Kent, D.V., Dia, O., Sougy, J., 1984. Paleomagnetism of lower-middle devonian rocks and upper proterozoic-cambrian(?) rocks from Mejeria (Mauritania West Africa). AGU Geodynam. Ser. 12, 99–115.

Kent, D.V., Smethurst, M.A., 1998. Shallow bias of paleomagnetic inclinations in the Paleozoic and Precambrian. Earth Planet. Sci. Lett. 160, 391–402.

Khattach, D., Robardet, M., Perroud, H., 1995. A Cambrian pole for the Moroccan coastal meseta. Geophys. J. Int. 120, 132–144.

Kilner, B., Mac Niocaill, C., Brasier, M., 2005. Low-latitude glaciation in the Neoproterozoic of Oman. Geology 433, 413–416.

Kirchvink, J.L., 1992. The late Proterozoic low latitude glaciation: the snowball Earth. In: Schopf, J.W., Klein, C. (Eds.), The Proterozoic Biosphere. Cambridge University Press, Cambridge, pp. 51–52.

Kirschvink, J.L., Ripperdan, R.L., Evans, D.A.D., 1997. Evidence for a large-scale reorganization of early Cambrian continental masses by inertial interchange true polar wander. Science 277, 541–545.

Kröner, A., 1977. Precambrian mobile belts of southern and eastern Africa-ancient suture or sites of ensialic mobility? A case for crustal evolution towards plate tectonics. Tectonophysics 40, 101–135.

Kröner, A., Correia, H., 1980. Continuation of the Pan-African Damara belt into Angola: a proposed correlation of the Chela Group in southern Angola with the Nosib Group in northern Namibia/SWA. Trans. Geol. Soc. S. Afr. 83, 5–16.

Kröner, A., McWilliams, M.O., Germs, G.J.B., Reid, A.B., Schalk, K.E.L., 1980. Paleomagnetism of late Precambrian to early Paleozoic Mixtite-Bearing formations in Namibia (South West Africa): the Nama Group and Blaubeker formation. Am. J. Sci. 280, 942–968.

Kröner, A., Cordani, U.G., 2003. African, southern Indian and South American cratons were not part of the Rondinia supercontinent: evidence from field relationships and geochronology. Tectonophysics 375, 325–352.

Laux, J.H., Pimentel, M.M., Dantas, E.L., Armstrong, R., Junges, S.L., 2005. Two neoproterozoic crustal accretion events in the Brasília belt, central Brazil. J. S. Am. Earth Sci. 18, 183–198.

Lawver, L., Scotese, C.R., 1987. A revised reconstruction of Gondwanaland. In: McKenzie, G.D. (Ed.), Gondwana Six: Structure, Tectonics and Geophysics. AGU Geophys. Mon. 40, 17–23.

Layer, P.W., Kröner, A., McWilliams, M., 1996. An Archean geomagnetic reversal in the Kaap Valley Pluton, South Africa. Science 273, 943–946.

Loewy, S.L., Connelly, J.N., Dalziel, I.W.D., Gower, C.F., 2003. Eastern Laurentia in Rodinia: constraints from whole-rock Pb and U/Pb geochronology. Tectonophysics 375, 169–197.

Machado, N., Valladares, C., Heilbron, M., Valeriano, C., 1996. U–Pb geochronology of the central Ribeira belt (Brazil) and implications for the evolution of the Brazilian Orogeny. Precam. Res. 79, 347–361.

Macouin, M., Besse, J., Ader, M., Gilder, S., Yang, Z., Sun, Z., Agrinier, P., 2004. Combined paleomagnetic and isotopic data from the Doushantuo carbonates, South China: implications for the "snowball Earth" hypothesis. Earth Planet. Sci. Lett. 224, 387–398.

Mare, L.P., Thomas, R.J., 1997. Palaeomagnetism and aeromagnetic modelling of the Mesoproterozoic Ntimbankulu Pluton, KwaZulu-Natal, South Africa; mushroom-shaped diapir? J. Afr. Earth Sci. 25, 519–537.

Martin, D.L., Nairn, A.E.M., Noltimier, H.C., Petty, M.H., Schmidt, T.J., 1978. Paleozoic and Mesozoic paleomagnetic results from Morocco. Tectonophysics 44, 91–114.

Mayer, A., Singiol, S., Morais, E., 2000. The Kunene gabbro-anorthosite complex: coalescence of crystal mush intrusions during the early Kibaran. AGU Trans. 81, 1248–1249.

McCausland, P.J.A., Hodych, J.P., 1998. Paleomagnetism of the 550 Ma Skinner Cove volcanics of western Newfoundland and the opening of the Iapetus Ocean. Earth Planet. Sci. Lett. 163, 15–29.

McElhinny, M.W., 1966. The palaeomagnetism of the Umkondo Lavas, eastern Southern Rhodesia. Geophys. J. Roy. Astron. Soc. 10, 375–381.

McElhinny, M.W., Opdyke, N.D., 1964. The paleomagnetism of the Precambrian dolerites of eastern Southern Rhodesa, an example of geologic correlation by rock magnetism. J. Geophys. Res. 69, 2465–2475.

McElhinny, M.W., Powell, C.McA., Pisarevsky, S.A., 2003. Paleozoic terranes of eastern Australia and the drift history of Gondwana. Tectonophysics 362, 41–65.

McWilliams, M.O., Kröner, A., 1981. Paleomagnetism and tectonic evolution of the Pan-African Damara Belt, Southern Africa. J. Geophys. Res. 86, 5147–5162.

Meert, J.G., 1999. Some perspectives on the assembly of Gondwana. In: Radhakrishna, T., Piper, J.D.A. (Eds.), The Indian Subcontinent and Gondwana: A Paleomagnetic and Rock Magnetic Perspective. Mem. Geol. Soc. India 44, 45–58.

Meert, J.G., 2003. A synopsis of events related to the assembly of eastern Gondwana. Tectonophysics 362, 1–40.

Meert, J.G., Torsvik, T.H., 2003. The making and unmaking of a supercontinent: Rodinia revisited. Tectonophysics 375, 261–288.

Meert, J.G., Van der Voo, R., Powell, C.M., Li, Z.X., McElhinny, M.W., Chen, Z., Symons, D.T.A., 1993. A plate-tectonic speed limit? Nature 363, 216–217.

Meert, J.G., Van der Voo, R., 1994. The Neoproterozoic (1000–540 Ma) glacial intervals: no more snowball Earth? Earth Planet Sci. Lett. 123, 1–13.

Meert, J.G., Van der Voo, R., 1996. Paleomagnetic and $^{40}Ar/^{39}Ar$ study of the Sinyai dolerite, Kenya: implications for Gondwana Assembly. J. Geol. 104, 131–142.

Meert, J.G., Eide, E.A., Torsvik, T.H., 1997. The Nama Group revisited. Geophys. J. Int. 129, 637–650.

Meert, J.G., Hargraves, R.B., Van der Voo, R., Hall, C.M., Halliday, A.N., 1994. Paleomagnetic and $^{40}Ar/^{39}Ar$ studies of late Kibaran intrusives in Burundi, East Africa: implications for late Proterozoic supercontinents. J. Geol. 102, 621–637.

Meert, J.G., Torsvik, T.H., 2004. Paleomagnetic constraints on Neoproterozoic "Snowball Earth" continental reconstructions. The Extreme Proterozoic: Geology, Geochemistry, and Climate. In: Jenkins, G.S., McMenamin, M.A.S., McKay, C.P., Sohl, L. (Eds.), AGU Geophysical Monograph Series 146., doi:10.1029/146GM01, pp. 5–11.

Meert, J.G., Van der Voo, R., Ayub, S., 1995. Paleomagnetic investigation of the Neoproterozoic Gagwe lavas and Mbozi complex, Tanzania and the assembly of Gondwana. Precam. Res. 74, 225–244.

Meert, J.G., Nédélec, A., Hall, C., Wingate, M.T.D., Rakotondrazafy, M., 2001. Paleomagnetism, geochronology and tectonic implications of the Cambrian-age Carion granite, Central Madagascar. Tectonophysics 340, 1–21.

Meert, J.G., Nedelec, A., Hall, C., 2003. The stratoid granites of central Madagascar: Paleomagnetism and further age constraints on Neoproterozoic deformation. Precam. Res. 120, 101–129.

Merrill, R.T., McFadden, P.L., 1995. Dynamo theory and paleomagnetism. J. Geophys. Res. 100, 317–326.

Montes-Lauar, C.R., Trompette, R., Melfi, A.J., Bellieni, G., De Min, A., Bea, A., Piccirillo, E.M., Affaton, P., Pacca, I.G., 1997. Panafrican Rb–Sr isochron ages of magmatic rocks from northern Cameroon. Preliminary results. In: South-American Symposium on Isotopic Geology, Campos do Jordão, São Paulo, Brazil, pp. 204–205 (extended abstracts).

Morel, P., 1981. Palaeomagnetism of a Pan-African diorite: a late Precambrian pole for western Africa. Geophys. J. Roy. Astr. Soc. 65, 493–503.

Morris, W.A., Carmichael, C.M., 1978. Paleomagnetism of some late Precambrian and lower Paleozoic sediments from L'Adrar de Mauritanie, West Africa. Can. J. Earth Sci. 15, 253–262.

Moussine-Pouchkine, A., Bertrand- Sarfati, J., 1997. Tectonosedimentary subdivisions in the Neoproterozoic to early Cambrian cover of the Taoudeni basin (Algeria-Mauritania-Mali). J. Afr. Earth Sci. 24, 425–443.

Mushayandebvu, M.F., Jones, D.L., Briden, J.C., 1994. A palaeomagnetic study of the Umvimeela Dike, Zimbabwe: Evidence for a mid-Proterozoic thermal overprint. Precam. Res. 69, 269–280.

Nairn, A.E.M., Perry, T.A., Ressetar, R., Rogers, S., 1987. A paleomagnetic study of the Dokhan Volcanic formation and younger granites, eastern desert of Egypt. J. Afr. Earth Sci. 6, 353–365.

Neves, S.P., 2003. Proterozoic history of the Borborema province (NE Brazil): correlations with neighboring cratons and Pan-African belts and implications for the evolution of western Gondwana. Tectonics 22, 1031, doi:10.1029/2001TC001352.

Nomade, S., Chen, Y., Pouclet, A., Féraud, G., Théveniaut, H., Daouda, B.Y., Vidal, M., Rigolet, C., 2003. The Guiana and the West African Shield Palaeoproterozoic grouping: new palaeomagnetic data for

French Guiana and the Ivory Coast. Geophys. J. Int. 154, 677–694.

Onstott, T.C., Hargraves, R.B., 1981. Proterozoic transcurrent tectonics: palaeomagnetic evidence from Venezuela and Africa. Nature 289, 131–136.

Onstott, T.C., Hargraves, R.B., Joubert, P., 1986a. Constraints on the tectonic evolution of the Namaqua province. II. Reconnaissance paleomagnetic and $^{40}$Ar–$^{39}$Ar results from the Namaqua province and Kheis belt. Trans. Geol. Soc. S. Afr. 89, 143–170.

Onstott, T.C., Hargraves, R.B., Reid, D.L., 1986b. Constraints on the tectonic evolution of the Namaqua province. III. Palaeomagnetic and $^{40}$Ar–$^{39}$Ar results from the Gannakouriep dike swarm. Trans. Geol. Soc. S. Afr. 89, 171–183.

Pedrosa-Soares, A.C., Vidal, P., Leonardos, O.H., Brito Neves, B.B., 1998. Neoproterozoic oceanic remnants in eastern Brazil: further evidence and refutation of an exclusively ensialic evolution for the Araçuaí-West Gongo orogen. Geology 26, 519–522.

Pedrosa-Soares, A.C., Noce, C.M., Wiedemann, C.M., Pinto, C.P., 2001. The Araçuaí-West Congo Orogen in Brazil: an overview of a confined orogen formed during Gondwanaland assembly. Precam. Res. 110, 307–323.

Perrin, M., 1994. Complex magnetization of the Early Cambrian Jolcano-Sedimentary sequence from the Bou Azzer region, Anti Atlas (Morocco). Phys. Earth Planet. Interiors 85, 35–51.

Perrin, M., Prévot, M., 1988. Uncertainties about Proterozoic and Paleozoic polar wander path of West African craton and Gondwana: evidence for sucessive remagnetization events. Earth Planet. Sci. Lett. 88, 337–347.

Perrin, M., Elston, D.P., Moussine-Pouchkine, A., 1988. Paleomagnetism of Proterozoic and Cambrian strata, Adrar de Mauritanie, cratonic West Africa. J. Geophys. Res. 93, 2159–2178.

Pesonen, L.J., Elming, S.-A., Pisarevsky, S., D'Agrella-Filho, M.S., Meert, J., Schmidt, P.W., Abrahansen, N., Bylund, G., 2003. Paleomagnetic configuration of continents during the Proterozoic. Tectonophysics 375, 289–324.

Pimentel, M.M., Fuck, R.A., 1992. Neoproterozoic crustal accretion in central Brazil. Geology 20, 375–379.

Pimentel, M.M., Fuck, R.A., Alvarenga, C.J.S., 1996. Post-Brasiliano (Pan-African) high-K granitic magmatism in Central Brazil: the role of late Precambrian-early Palaeozoic extension. Precam. Res. 80, 217–238.

Pimentel, M.M., Fuck, R.A., Jost, H., Ferreira-Filho, C.F., Araújo, S.M., 2000. The basement of the Brasília fold belt and the Goiás magmatic arc. In: Cordani, U.G., Milani, E.J., Thomaz Filho, A., Campos, D.A. (Eds.), Tectonic Evolution of South America, 31st International Geological Congress. Rio de Janeiro, Brazil, pp. 195–229.

Pinna, P., Cocherie, A., Thieblemont, D., Jezequel, P., 2000. The Kisii Group of western Kenya: an end-Archaean (2.53 Ga) late orogenic volcano sedimentary sequence. J. Afr. Earth Sci. 30, 79–97.

Piper, J.D.A., 1972. A palaeomagnetic study of the Bukoban system, Tanzania. Geophys. J. Roy Astr. Soc. 28, 111–127.

Piper, J.D.A., 1974. Magnetic properties of the Cunene anorthosite complex, Angola. Phys. Earth Planet. Inter. 9, 353–363.

Piper, J.D.A., 1975. Palaeomagnetic correlations of Precambrian formations of east-central Africa and their tectonic implications. Tectonophysics 26, 135–161.

Piper, J.D.A., 1976. Paleomagnetic evidence for a Proterozoic supercontinent. Phil. Trans. Roy. Soc. Lond. 280, 469–490.

Piper, J.D.A., 1980. Analogous Upper Proterozoic apparent polar wander loops. Nature 283, 845–847.

Piper, J.D.A., 1983. Dynamics of the continental crust in Proterozoic times. Geol. Soc. Am. Mem. 161, 11–34.

Piper, J.D.A., 2000. The Neoproterozoic supercontinent: Rodinia or Palaeopangaea. Earth Planet. Sci. Lett. 176, 131–146.

Pisarevsky, S.A., Komissarova, R.A., Khramov, A.N., 2001. Reply to the comment of J.G. Meert and R. Van der Voo "New palaeomagnetic results from Vendian red sediments in Cisbaikalia and the problem of the relationship of Siberia and Laurentia in the Vendian". Geophys. J. Int. 146, 871–873.

Pisarevsky, S.A., Wingate, M.T.D., Powell. C.McA., Johnson, S., Evans, D.A.D., 2003. Models of Rodinia Assembly and Fragmentation. In: Yoshida, M., Windley, B.F., Dasgupta, S. (Eds.), Proterozoic East Gondwana: Supercontinent Assembly and Breakup. Geol. Soc. Sp. Pub. 206, 35–55.

Ponte-Neto, C.F., 2001. Contribuição ao estudo da Formação do Gondwana Ocidental: Novos dados paleomagnéticos. PhD Thesis. IAG-USP, São Paulo, Brazil, pp. 106.

Powell, C.Mc.A., Jones, D.L., Pisarevsky, S.A., Wingate, M.T.D., 2001. Paleomagnetic constraints on the position of the Kalahari craton in Rodinia. Precam. Res. 110, 33–46.

Refai, E., Wassif, N.A., Shoaib, A., 1989. Stability of remanence and paleomagnetic studies of some chromite ores from Barramiya and Allawai occurrences, eastern Desert. Egypt Earth Planet. Sci. Lett. 94, 151–159.

Reid, A.B., 1968. A palaeomagnetic study of the Sijarira Group, Rhodesia. MPhil Thesis. University of London, 67 p.

Reid, D.L., Ransome, I.G.D., Onstott, T.C., Adams, C.J., 1991. Time of emplacement and metamorphism of late Precambrian mafic dikes associated with the Pan-African Gariep orogeny, Southern Africa: implications for the age of the Nama Group. J. Afr. Earth Sci. 13, 531–541.

Reischmann, T., Bachtadse, V., Kröner, A., Layer, P.W., 1992. Geochronology and paleomagnetism of a late Proterozoic island arc terrane from the Red sea hills, NE Sudan. Earth Planet. Sci. Lett. 114, 1–15.

Renne, P.R., Onstott, T.C., D'Agrella-Filho, M.S., Pacca, I.G., Teixeira, W., 1990. $^{40}$Ar–$^{39}$Ar dating of 1.0–1.1 Ga magnetizations from the São Francisco and Kalahari Cratons: tectonic implications for Pan-African and Brasiliano mobile belts. Earth Planet. Sci. Lett. 101, 349–366.

Restrepo-Pace, P.A., Ruiz, J., Gehrels, G., Cosca, M.A., 1997. Geochronology and Nd isotopic data of Grenville-age rocks in the Colombian Andes: new constraints for late Proterozoic–early Paleozoic paleocontinental reconstructions of the Americas. Earth Planet. Sci. Lett. 150, 427–441.

Sadowski, G.S., Bettencourt, J.S., 1996. Mesoproterozoic tectonic correlations between eastern Laurentia and the western border of the Amazon Craton. Precam. Res. 76, 213–227.

Sánchez-Bettucci, L., Rapalini, A.E., 2002. Paleomagnetism of the Sierra de Las Animas Complex, southern Uruguay: its implications in the assembly of western Gondwana. Precam. Res. 118, 243–265.

Saradeth, S., Soffel, H.C., Horn, P., Muller-Sohnius, D., Schult, A., 1989. Upper Proterozoic and Phanerozoic pole positions and Potassium–Argon (K–Ar) ages from the East Sahara craton. Geophys. J. Int. 97, 209–221.

Saylor, B.Z., Grotzinger, J.P., Germs, G.J.B., 1995. Sequence stratigraphy and sedimentology of the Neoproterozoic Kuibis and Schwarzrand Subgroups (Nama Group), southwestern Namibia. Precam. Res. 73, 153–171.

Schmitt, R.S., Trouw, R.A.J., Van Schmus, W.R., Pimentel, M.M., 2004. Late amalgamation in the central part of West Gondwana: new geochronological data and the characterization of a Cambrian collisional orogeny in the Ribeira Belt (SE Brazil). Precam. Res. 133, 29–61.

Stern, R.J., 1994. Arc assembly and continental collision in the Neoproterozoic East African orogen: implications for the consolidation of Gondwanaland. Ann. Rev. Earth Planet. Sci. 22, 319–351.

Stoesser, D.B., Camp, V.E., 1985. Pan-African microplate accretion of the Arabian shield. Geol. Soc. Am. Bull. 96, 817–826.

Tack, L., Wingate, M.T.D., Liégeois, J.-P., Fernandez-Alonso, M., Deblond, A., 2001. Early Neoproterozoic magmatism (1000–910 Ma) of the Zadinian and Mayumbian Groups (Bas-Congo): Onset of Rodinia rifting at the western edge of the Congo craton. Precam. Res. 110, 277–306.

Tahon, A., Fernandez-Alonso, M., Tack, L., Barrit, S.D., 2004. New insights about the evolution of the Mesoproterozoic Northeastern Kibaran belt (Central Africa). Abstracts. In: Proceedings of the 20th Colloquium of African Geology, Orleans, France.

Tohver, E., van der Pluijm, B.A., Van der Voo, R., Rizzotto, G., Scandolara, J.E., 2002. Paleogeography of the Amazon craton at 1–2 Ga: early Grenvillian collision with the Llano segment of Laurentia. Earth Planet. Sci. Lett. 199, 185–200.

Tohver, E., van der Pluijm, B.A., Mezger, K., Scandolara, J.E., Essene, E.J., 2004a. Significance of the Nova Brasilândia Metasedimentary Belt in western Brazil: redefining the Mesoproterozoic boundary of the Amazon craton. Tectonics 23, TC6004, doi:10.1029/2003TC001563.

Tohver, E., Bettencourt, J.S., Tosdal, R., Mezger, K., Luis, W.B., Payolla, B., 2004b. Pb isotopes and tectonic affinities of the Grenville-deformed Amazon basement: Terrane transfer with southern Laurentia? Earth Planet. Sci. Lett. 228, 161–176, doi:10.1016/j.epsl.2004.09.029.

Tohver, E., Trindade, R.I.F., Font, E., 2004c. Bending or buckling of a Brasiliano belt: a paleomagnetic investigation of the curvature of the Paraguai belt (SW Brazil) and implications for Neoproterozoic/Cambrian tectonics of western Gondwana. In: Proceedings of the AGU Fall Meeting, San Francisco.

Tohver, E., van der Pluijm, B.A., Mezger, K., Scandolara, J.E., Essene, E.J., 2005a. Two stage tectonic history of the SW Amazon craton in the late Mesoproterozoic: identifying a cryptic suture zone. Precam. Res. 137, 35–59.

Tohver, E., van der Pluijm, B.A., Scandolâra, J.E., Essene, E.J., 2005b. Grenville-aged deformation of Amazonia (Rondônia, Brazil): evidence for collision with southern Laurentia. J. Geol. 113, 309–323.

Torquato, J.R., Cordani, U.G., 1981. Brazil-Africa geological links. Earth Sci. Rev. 17, 155–176.

Torsvik, T.H., Carter, L.M., Ashwal, L.D., Bhushan, S.K., Pandit, M.K., Jamtveit, B., 2001. Rodinia refined or obscured: Palaeomagnetism of the Malani Igneous Suite (NW India). Precam. Res. 108, 319–333.

Trindade, R.I.F., 1999. Magnetismo de corpos graníticos e a evolução tectônica brasiliana da porção ocidental da faixa Seridó (NE do Brasil). PhD Thesis. IAG-USP, São Paulo, pp. 198.

Trindade, R.I.F., Font, E., D'Agrella-Filho, M.S., Nogueira, A.C.R., Riccomini, C., 2003. Low-latitude and multiple geomagnetic reversals in the Neoproterozoic Puga cap carbonate, Amazon craton. Terra Nova 15, 441–446.

Trindade, R.I.F., D'Agrella-Filho, M.S., Babinski, M., Font, E., Brito-Neves, B.B., 2004. Paleomagnetism and geochronology of the Bebedouro cap carbonate: evidence for continental-scale cambrian remagnetization in the São Francisco craton, Brazil. Precam. Res. 128, 83–103.

Trindade, R.I.F., D'Agrella-Filho, M.S., Epof, I., Brito-Neves, B.B., 2006. Paleomagnetism of the early Cambrian Itabaiana mafic dikes, NE Brazil, and implications for the final assembly of Gondwana and its proximity to Laurentia. Earth Planet. Sci. Lett., in press.

Trompette, R., 2000. Gondwana evolution, its assembly at around 600 Ma. Comptes Rendus de l'Academie des Ciences Serie II. Fascicule A—Sciences de la Terre et des Planetes, 330, pp. 305–315.

Valeriano, C.M., Machado, N., Simonetti, A., Valladares, C.S., Seer, H.J., Simões, L.S.A., 2004. U–Pb geochronology of the southern Brasília belt (SE-Brazil): Sedimentary provenance, Neoproterozoic orogeny and assembly of West Gondwana. Precam. Res. 20, 27–55.

Valencio, D.A., Sinito, A.M., Vilas, J.F., 1980. Palaeomagnetism of Upper Precambrian rocks of the La Tinta Formation. Argent. Geophys. J. Roy Astr. Soc. 62, 563–575.

Van der Voo, R., 1990. The reliability of paleomagnetic data. Tectonophysics 184, 1–9.

Van der Voo, R., Meert, J.G., 1991. Late Proterozoic paleomagnetism and tectonic models: a critical appraisal. Precam. Res. 53, 149–163.

Villeneuve, M., Cornée, J.J., 1994. Structure, evolution, and paleogeography of the West African craton and bordering belts during the Neoproterozoic. Precam. Res. 69, 307–326.

Weil, A.B., Van der Voo, R., Niocaill, C.M., Meert, J.G., 1998. The Proterozoic supercontinent Rodinia: Paleomagnetically derived reconstructions for 1100–800 Ma. Earth Planet. Sci. Lett. 154, 13–24.

Weil, A.B., Van der Voo, R., van der Pluijm, B., 2001. New paleomagnetic data from the southern Cantabria-Asturias Arc, northern Spain: implications for true oroclinal rotation and the final amalgamation of Pangea. Geology 29, 991–994.

Wilde, S.A., Youssef, K., 2000. Significance of SHRIMP U–Pb dating of the imperial Porphyry and associated Dokhan Volcanics, Gebel Dokhan, north Eastern Desert, Egypt. J. Afr. Earth Sci. 31, 403–413.

Williams, G.E., Schmidt, P., 2000. Proterozoic equatorial glaciation: has 'snowball Earth' a snowball's chance? Aust. Geol. 117, 21–25.

Windley, B.F., Whitehouse, M.J., Ba-Bttat, M.A.O., 1996. Early Precambrian gneisses and Pan-African island arcs in Yemen: crustal accretion of the eastern Arabian shield. Geology 24, 131–134.

Wingate, M.T.D., 2001. SHRIMP baddeleyite and zircon ages for an Umkondo dolerite sill, Nyanga Mountains, Eastern Zimbabwe. S. Afr. J. Geol. 104, 13–22.

Wingate, M.T., Pisarevsky, S.A., De Waele, B., 2004. Paleomagnetism of the 765 Ma Luakela Volcanics in NW Zambia and implications for Neoproterozoic Positions of the Congo Craton, EOS Transaction. In: AGU, 85 (47) Fall Meeting, San Francisco.

Yu, Y., Dunlop, D.J., 2002. Multivectorial paleointensity determination from the Cordova Gabbro, southern Ontario. Earth Planet. Sci. Lett. 203, 983–998.